STUDY OF GAMMA RAYS FROM NEUTRON INELASTIC SCATTERING

by

Bertram H. Hui
Norman C. Rasmussen

Department of Nuclear Engineering
Massachusetts Institute of Technology
Cambridge, Massachusetts 02139

MITNE-112
Contract No. H0180895

February 1970

Prepared for

United States Department of the Interior
Bureau of Mines
Morgantown Research Center
Morgantown, West Virginia

ABSTRACT

The energy and intensity of the inelastic gamma rays of twenty low atomic number elements: Li, C, N, O, Mg, Al, Na, Si, S, Cl, K, Ti, V, Cr, Mn, Fe, Co, Ni, Cu, and Pb, are measured with a 30 cc Ge(Li) detector using an unmoderated 5 curie Pu-Be neutron source. The value of the production cross section for the Pu-Be spectrum is calculated. The results show they are mostly less than one barn.

TABLE OF CONTENTS

LIST OF FIGURES

LIST OF FIGURES (Contd)

List of Tables

Acknowledgements

I would like to express my deepest appreciation to all those who had helped in this work, especially to my supervisor, Prof. N.C. Rasmussen, for his valuable guidance throughout this work and for his unlimitted patience in correcting this thesis.

I wish to thank especially Dr. J.N. Hamawi and Dr. T.L. Harper Jr. for their help in computer analysis and in setting up the experimental apparatus.

Acknowledgement is made to the U.S. Bureau of Mines for supporting funds for the project.

Chapter I

INTRODUCTION

The work in this thesis is aimed at determining the energy and intensity of gamma rays produced by the inelastic scattering of fast neutrons by a series of elemental samples. The fast neutrons used were obtained from a 5 Ci Pu-Be source. The gamma rays were detected with a 30 c.c. Ge(Li) detector. The work was supported by the U. S. Bureau of Mines to provide a useful basic data to help evaluate the potential of these gamma rays for determing the isotopic content of large inhomogeneous process streams of the type often encountered in the mining industry.

The analysis of large volume inhomogeneous streams is a difficult problem by ordinary analysis methods because it is very hard to get a representative sample. The advantage of using fast neutrons and high energy gamma rays is that both radiations are highly penetrating and so it is possible in principal to get a measurement if the average content of several cubic feet thus greatly reducing the sampling error. Further if appropriately large sources of neutrons are used, this analysis can be done rapidly enough so that the measurement can be done on a moving process stream.

Recognizing this, the U.S. Bureau of Mines has been investigating this technique in recent years(ref. 1) using an (α,n) neutron source and a NaI gamma ray detector. The relatively poor energy resolution of NaI does not permit the complete resolution of the gamma rays emitted. Its relatively high detection efficiency however makes it the only practival detector for this application at this time.

In this study we have used a Ge(Li) detector to measure the gamma rays. This detector has an energy resolution about a factor of 10 better than NaI but unfortunately its efficiency is considerably poorer. The data obtained with this improved resolution can be used to determine which elements might interfere with each other when NaI is used. The data can further be used in many cases to make appropriate corrections when it is determined that inteference has occured.

In this work the energy and intensity of the inelastic gamma rays of some 20 low atomic number elements: Li, C, N, O, Mg, Al, Na, Si, S, Cl, K, Ti, V, Cr, Mn, Fe, Co, Ni, Cu, and Pb, have been measured. The intensities have also been used to calculate the gamma ray production cross section using the geometric and intrinsic efficiencies of the system.

Chapter II describes the basic theory involved, in Chapter III the equipment and procedures are described. In Chapter IV, the data reduction method used is described and the final results are given. Conclusion is given in Chapter V.

Chapter II

THEORY

2.1 The Inelastic Scattering Process

In neutron inelastic scattering, a fast neutron strikes a nucleus and raises it to an excited state. The neutron is scattered with energy E_n' less than its initial energy E_n and the nucleus de-excites and gives out gamma ray of energy (if the recoil energy of the nucleus is ignored)

$$h\nu = E_n - E_n' \qquad (2.1)$$

The energies of these gamma rays are related to the nuclear level structure of the nuclei found in the sample, and are different for each nuclear species. This gives, in theory, an unambiguous determination of the major elements present, since the relative proportion of gamma rays of different energies is directly related to the relative abundance of the various elements present in the sample.

For very light elements, however, fast neutron inelastic scattering becomes less important because their level spacings are large and also because the neutrons are quickly moderated. Because of the neutron moderation, the dominate gamma rays in low Z materials are usually produced by neutron capture. Nevertheless, if the sample is so thin that moderation is negligible, then fast neutron inelastic scattering will

be the primary process. For medium and high atomic number elements, the levels spacings are quite close and elastic scattering does not slow the neutrons so quickly and the gamma rays from inelastic scattering become dominent.

A typical gamma ray spectrum of plate geometry using a 5 curie Pu-Be source shown in page 33. The characteristic energies of nucleus species stands out as peaks and they are mostly from neutron inelastic scattering. The area (in counts) under each peak is proportional to the intensity of that gamma energy reaching the detector. It is possible to relate the intensity to the production cross section of this energy. The following is the approximate method used to determine the production cross section for the slab geometry used.

2.2 Calculation of Production Cross Section for Slab Geometry

The plate geometry is shown in Figure 2.1. The neutron flux reaching the plate per unit area is

$$\phi = \frac{\phi_o}{4\pi l_s^2} \qquad (2.2)$$

Where ϕ_o = the strength of the neutron source

l_s = distance between the source and the unit area

The number of inelastic gamma rays produced per sec. per unit volume with energy E at the plate is

$$P = \phi N \sigma \qquad (2.3)$$

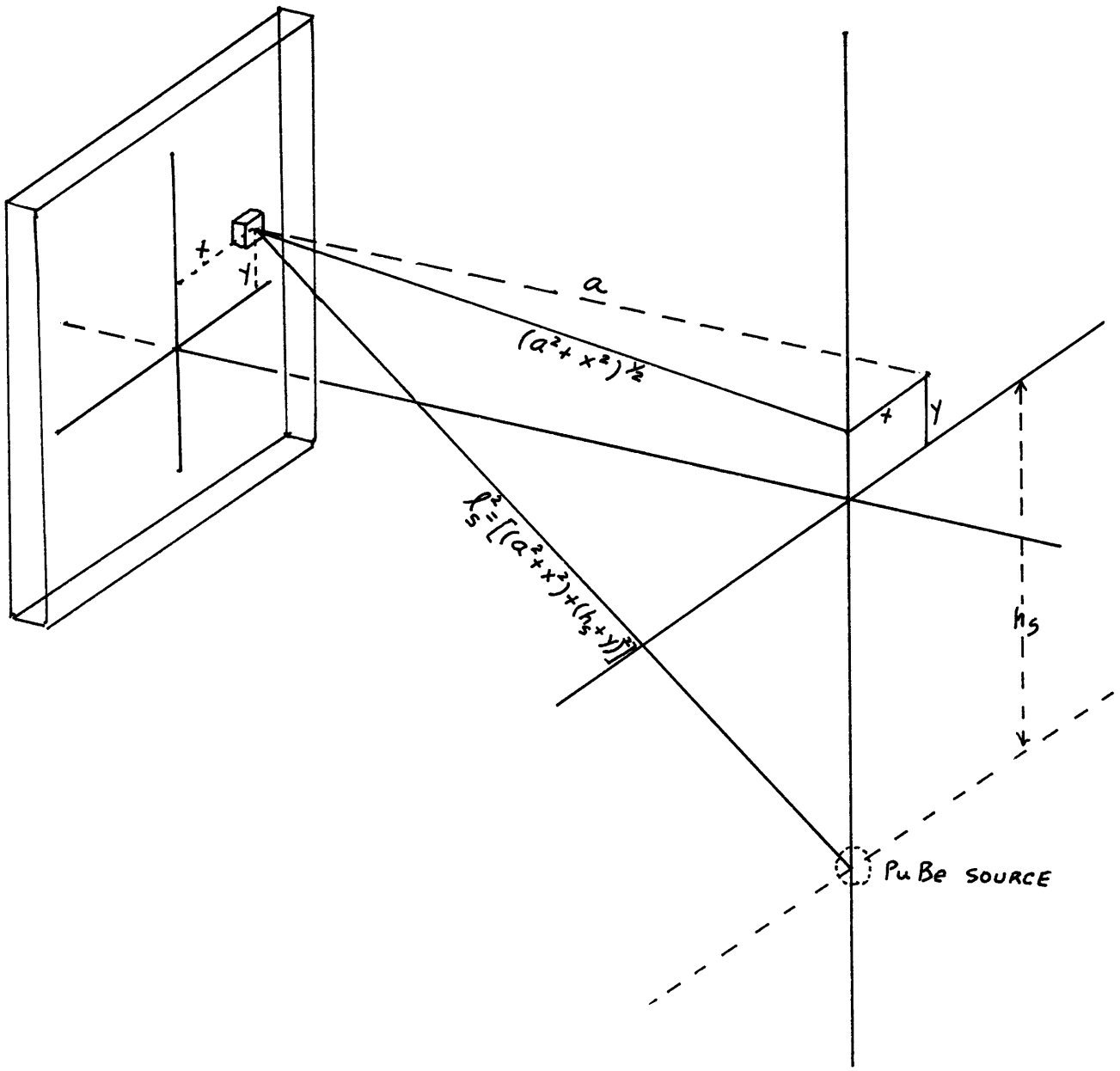

Figure 2.1 Slab Geometry For Calculating Production Cross Section

where N = atomic density of the material (atoms/c.c.)

σ = photon production cross section (cm^2)

Total number of inelastic gamma of energy E emitted from the whole plate per sec is

$$P_T = \iint_{\substack{\text{WHOLE}\\ \text{PLATE}}} \frac{\phi_0 N \sigma t}{4\pi l_s^2} dx dy \qquad (2.4)$$

where t is the thickness of the plate.

Let the detector overall efficiency be defined as:

$$\epsilon = \frac{\text{number of counts measured per sec}}{\text{number of photons produced per sec}} \qquad (2.5)$$

Then the number of counts registered by the detector per sec. is

$$P_D = P_T \epsilon \qquad (2.6)$$

For two plates we have

$$P_D = 2\epsilon \iint \frac{\phi_0 N \sigma t}{4\pi l_s^2} dx dy \qquad (2.7)$$

$$P_D = \frac{\epsilon \phi_0 N \sigma t}{2\pi} \iint \frac{dx dy}{l_s^2} \qquad (2.8)$$

$$\sigma \approx \frac{2\pi P_D}{\epsilon \phi_0 N t \iint \frac{dx dy}{l_s^2}} \qquad (2.9)$$

In practice, the integral in equation (2.9) is not easy to evaluate, therefore we make the reasonable assumption

that l_s is constant and l_s equal the distance between the source and the center of the plate, then

$$\sigma \approx \frac{2\pi \rho_b l_s^2}{\epsilon \phi_0 N V} \qquad (2.10)$$

where V is the volume of the plate.

Simonson erronously equated $P\Omega/M$ to I(ref. 2, page 30, last two equations), where

P = number of photons produced in the entire sample per sec.

Ω = solid angle of the detector

M = total mass of the sample

He defined efficiency ϵ as:

$$\epsilon = \frac{\text{measured intensity of the entire sample}}{\text{intensity produced by the entire sample}} \qquad (2.11)$$

His calculation of I was obtained from:

$$I = \frac{\text{measured intensity (counts/gmxsec)}}{\epsilon} \qquad (2.12)$$

so I = number of photons produced per sec by one gram of sample

That is, the correct relation should be

$$I = P/M \qquad (2.13)$$

So the production cross section should be

$$\sigma = \frac{I A}{(A_v)\phi} \qquad (2.14)$$

where

A = atomic number

Av = Avogadro's number

ϕ = neutron flux at the plate (neutron/cm^2 x sec)

After a few substitutions, equation (2.14) will yield equation (2.10).

2.3 The Pu-Be Neutron Source

The fast neutron source used in these measurements was a 5 Ci Pu-Be mixture. The neutrons are produced by α bombardment of the Be by the following reaction

$$_4Be^9 + {}_2He^4 \longrightarrow {}_6C^{12} + {}_0n^1 + 5.7 \text{ MEV}$$

part of the time the $_6C^{12}$ is formed in the excited state giving

$$_4Be^9 + {}_2He^4 \longrightarrow {}_6C^{12*} + {}_0n^1 + 1.29\text{MEV}$$

$$_6C^{12*} \longrightarrow {}_6C^{12} + 4.43 \text{ MEV}$$

so that the neutron source produces a 4.43 MEV gamma ray characteristic of $_6C^{12}$ which is present in all spectra. The effect of this gamma ray is reduced by using 5" of lead between the source and detector in the experimental setup used in this work.

The radioactive material occupies about two thirds of the internal volume of tantalum container of 0.98 inches outer diameter, 0.1 inches thick and 1.25 inches tall. The whole container is fitted inside a stainless

steel bottle.

A spectrum of neutron energy distribution from the Pu-Be source is shown in figure **2.2** . Notice that it has three main energy groups: 1 MEV, 4 MEV and 7 MEV for which the 4 MEV group has the highest flux. The source gives 8×10^{6} neutrons per sec.

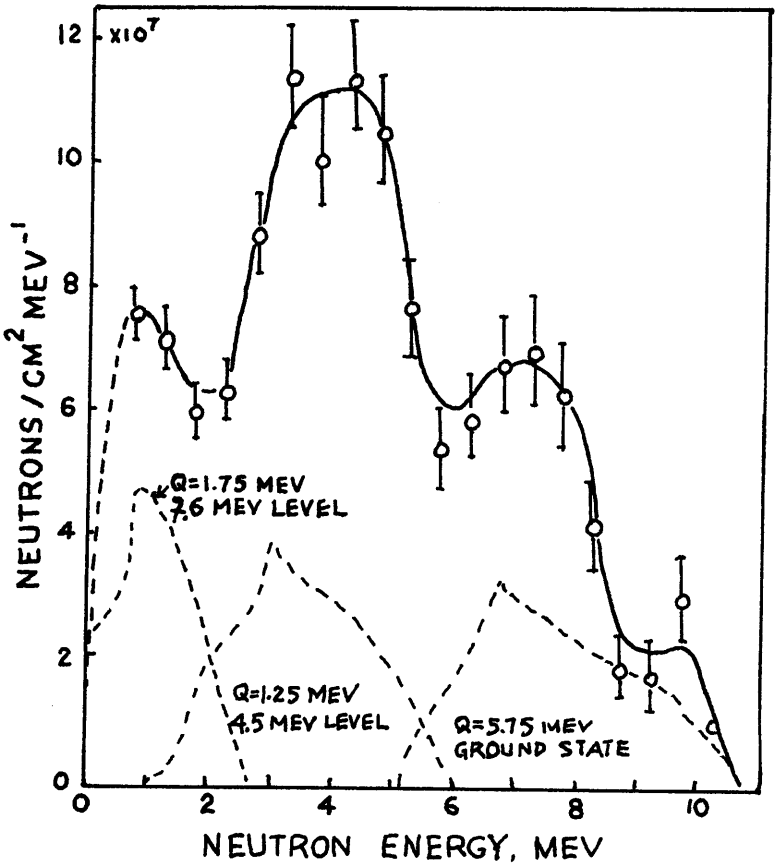

Figure 2.2 Energy Spectrum of The 5 Ci Pu-Be Source

Chapter III

EQUIPMENTS AND EXPERIMENTAL PROCEDURE

3.1 Gamma Ray Spectrometer

The gamma ray spectrometer system used in this work is similar to the one described by Orphan et al(ref. 3) A block diagram of the system is given in Figure 3.1

The gamma rays produced by neutron interactions are detected by a large coaxial lithium-drifted germanium detector. A detector bias voltage of 600 volts is supplied by a Canberra High Voltage Bias Supply (Model 3001). The preamplifier is a Canberra (Model 1408C) and is used in conjuction with Canberra Spectroscopy Amplifier (Model 1417) and pulse shaper. Pulses from the detector are analyzed and recorded with a 4096 channel Nuclear Data Analyzer (Model 161F). By ultilizing 4096 channels, it is possible to analyze gamma spectra from 0 to 8 MEV in one run with approxiately 2 KEV per channel. The data from the 4096 channel analyzer are punched out in paper tape by a Tally output unit (Model 406). The tapes are then converted to IBM cards. The whole data deck is then analyzed with the computer code GAMANL described in Chapter IV.

The germanium detector used in this work is a large coaxial type detector with an active volume of approximately 30 c.c. It was fabricated at the Massachusetts Institute

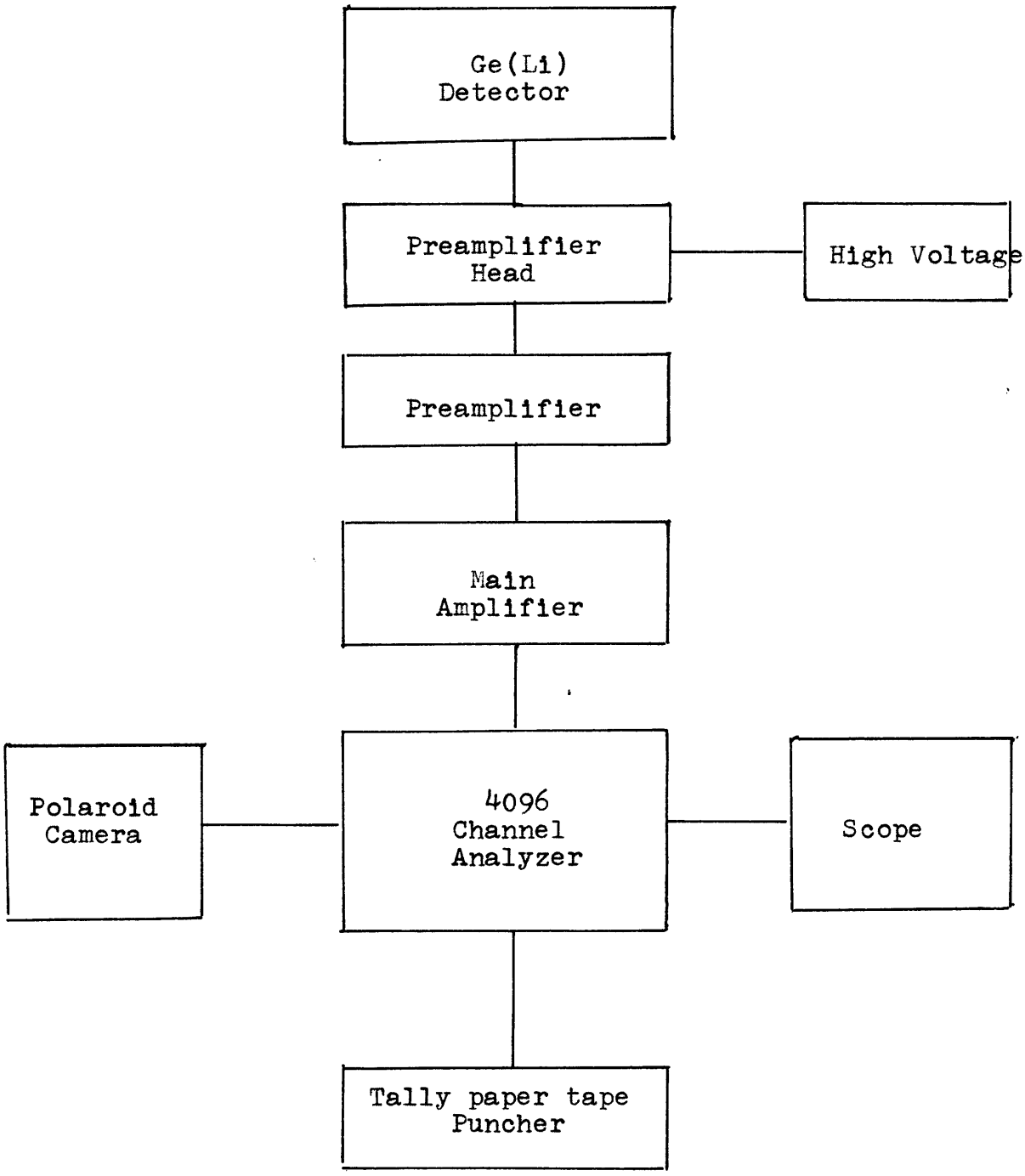

Figure 3.1 Block Diagram of The Gamma Spectrometer

of Technology in late 1966. The fabrication procedures and characteristics of Ge(Li) detectors which have been produced at M.I.T. are discussed in detail by Orphan and Rasmussen in reference (3). The actual detector was installed in a "snout" of liquid nitrogen cooled dewar, and was fastened to a copper "cold finger" which extended from the main dewar to the end of the snout.

Orphan and Rasmussen concluded that within the accuracies of their measurement (0.1% at 1 MEV and 0.01 % at 10 MEV), the Ge(Li) detector was linear over the energy range of 0.1 to 11 MEV. The efficiency of the detector system was determined by Simonson(ref. 2) and the efficiency curve is shown in Figure 3.2 .

Because of some small nonlinearities in the electronics a nonlinearity correction is required. This is accomplished using a high precision D.C. voltage standard Electronic Development Corporation (Model MV 100) with an absolute accuracy at one part in 10^4 and a mercury relay pulser are used to produce standard pulses for the linearity check. The test pulses are inserted in the preamplifier input with a uniform voltage spacing (approximately 40 channels between pulses). Deviations from linearity are then calculated from the resulting "spectrum". The linearity deviations of the system have been found to be constant over a period time.

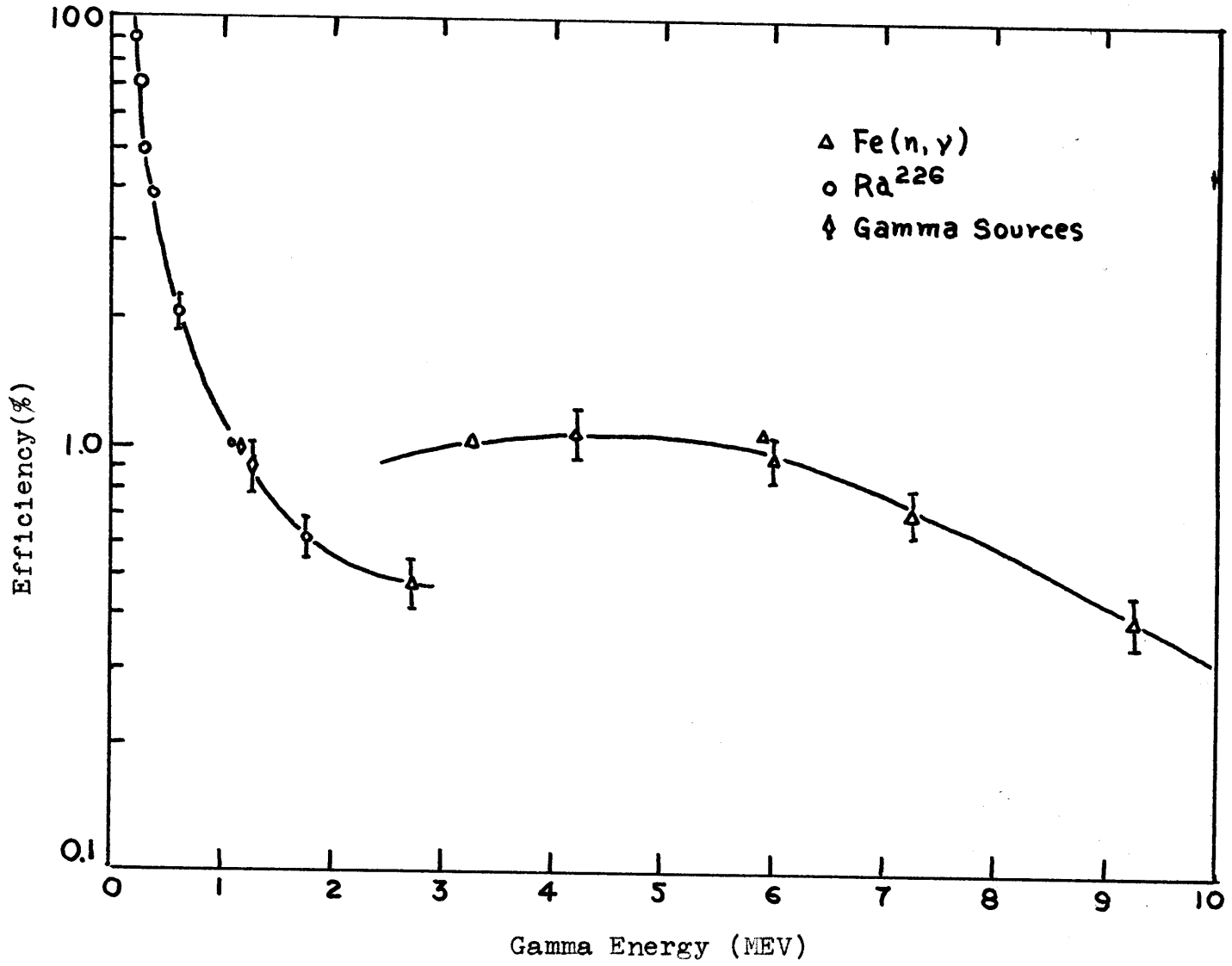

Figure 3.2 Detector Efficiency

3.2 Measurement Procedure

In order to measure the gamma rays from neutron inelastic scattering of different elements, an apparatus shown in figures 3.3, 3.4, 3.5 was used. The table supporting the detector and the source was made of aluminum. The samples to be studied were hung from two sides next to the fast neutron source. Their position relative to the source was optimised for highest count rate. The average count rate for stainless steel sample, for example, was about 260,000 counts per min.

The regular samples (stainless steel, aluminum, carbon, lead and glass) were in the form of plates (8" x 8" x ½"). The powder, liquid and scrap samples (lithium chloride, ammonium nitrate, magnesium, sodium chloride, sulphur, potassium chloride, titanium, vanadium, chromium oxide, manganese, cobalt, nickle, copper) were contained in aluminum cans of the same size.

A lead shield of 5 inches long and 2 inches diameter was placed between the fast neutron source and the gamma ray detector to prevent gamma rays from the source hitting the detector directly. The size of the lead block was optimised. Too large a lead shield would produce more background gamma by inelastic scattering than they eliminated. Too small a lead shield would be insufficient to protect the detector from being damaged.

When filling the powder sample, the cans had to be tapped regularly to assure uniform density. This is not

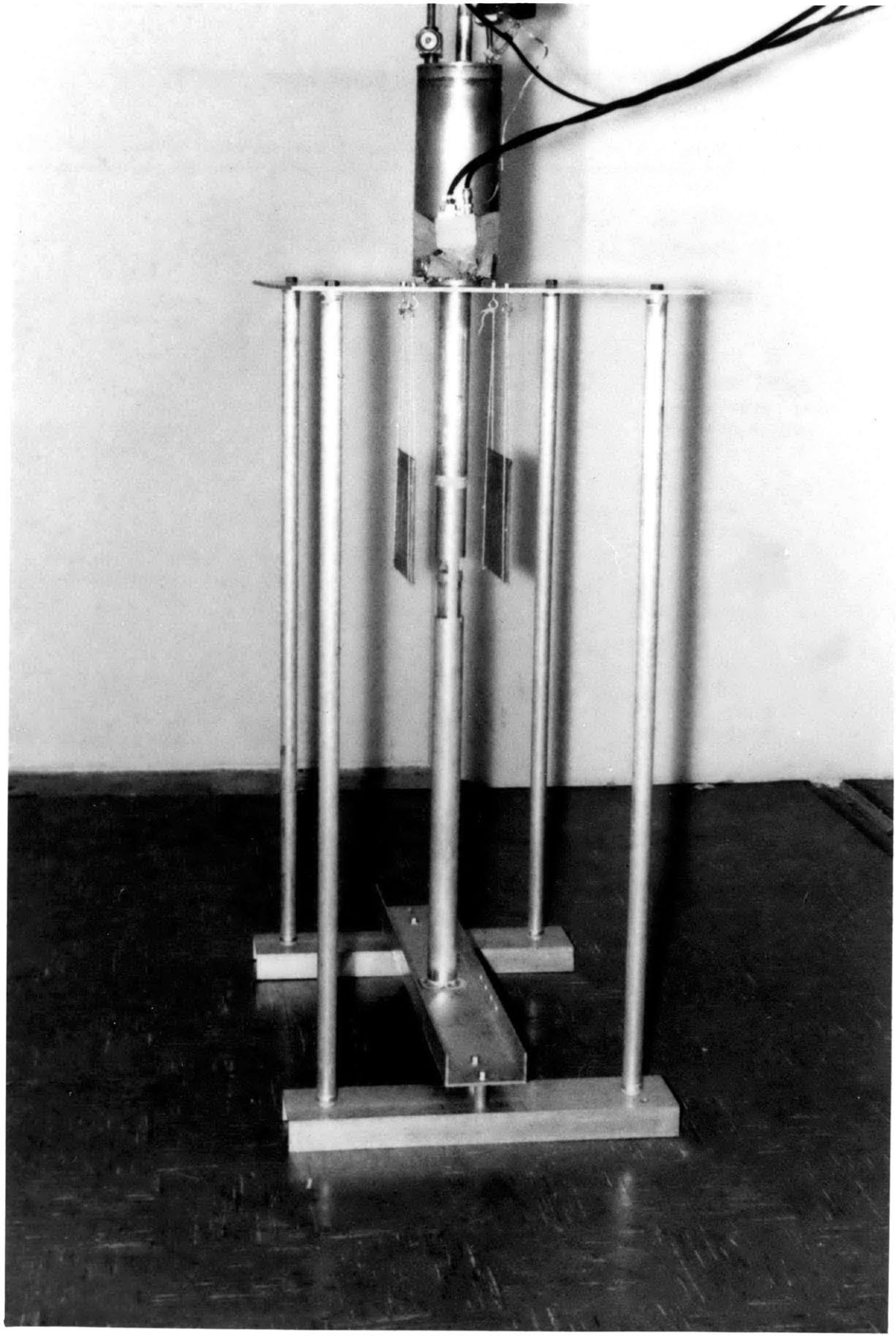

Figure 3.3 Experimental Setup

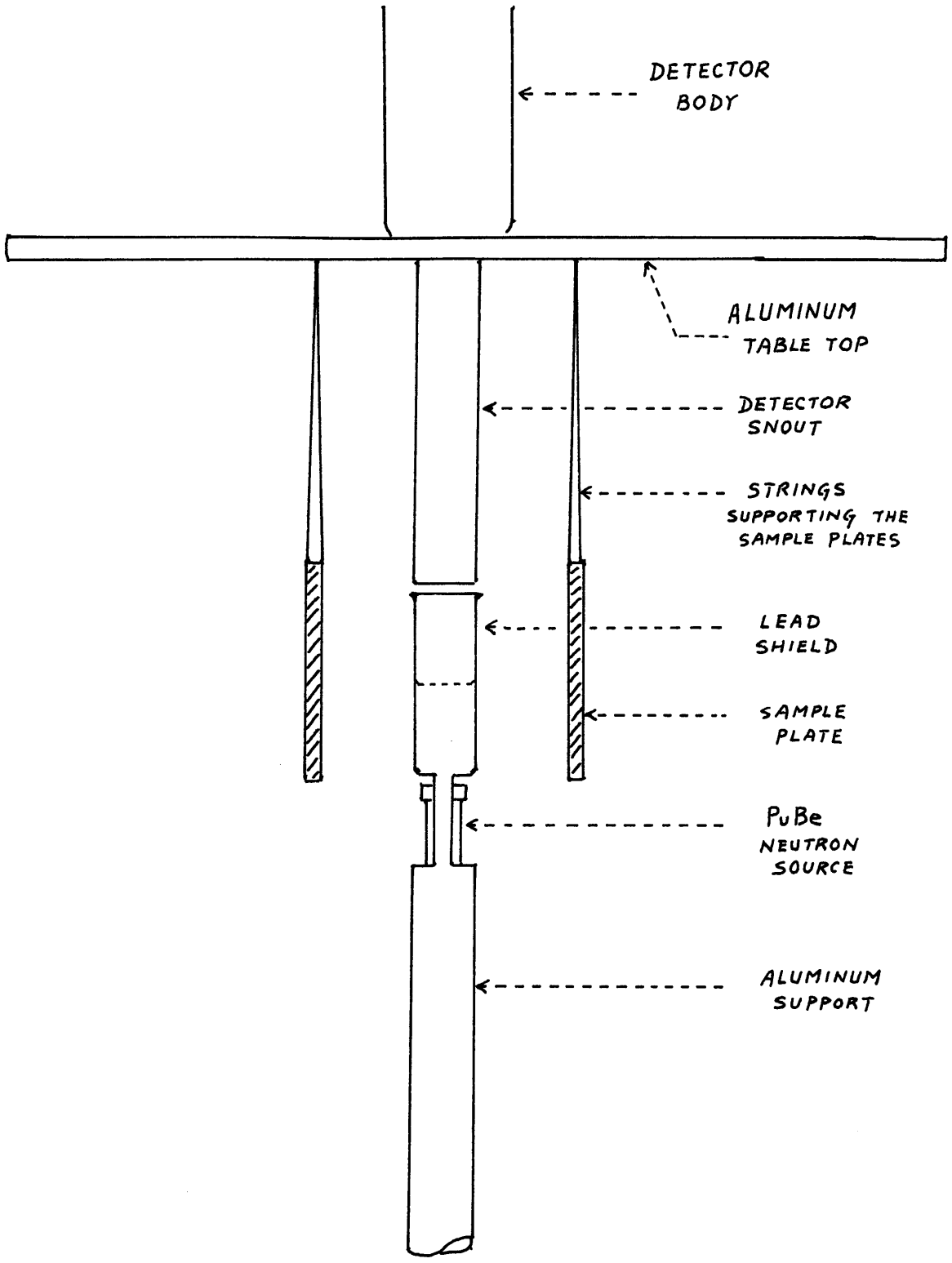

Figure 3.4 Experimental Setup

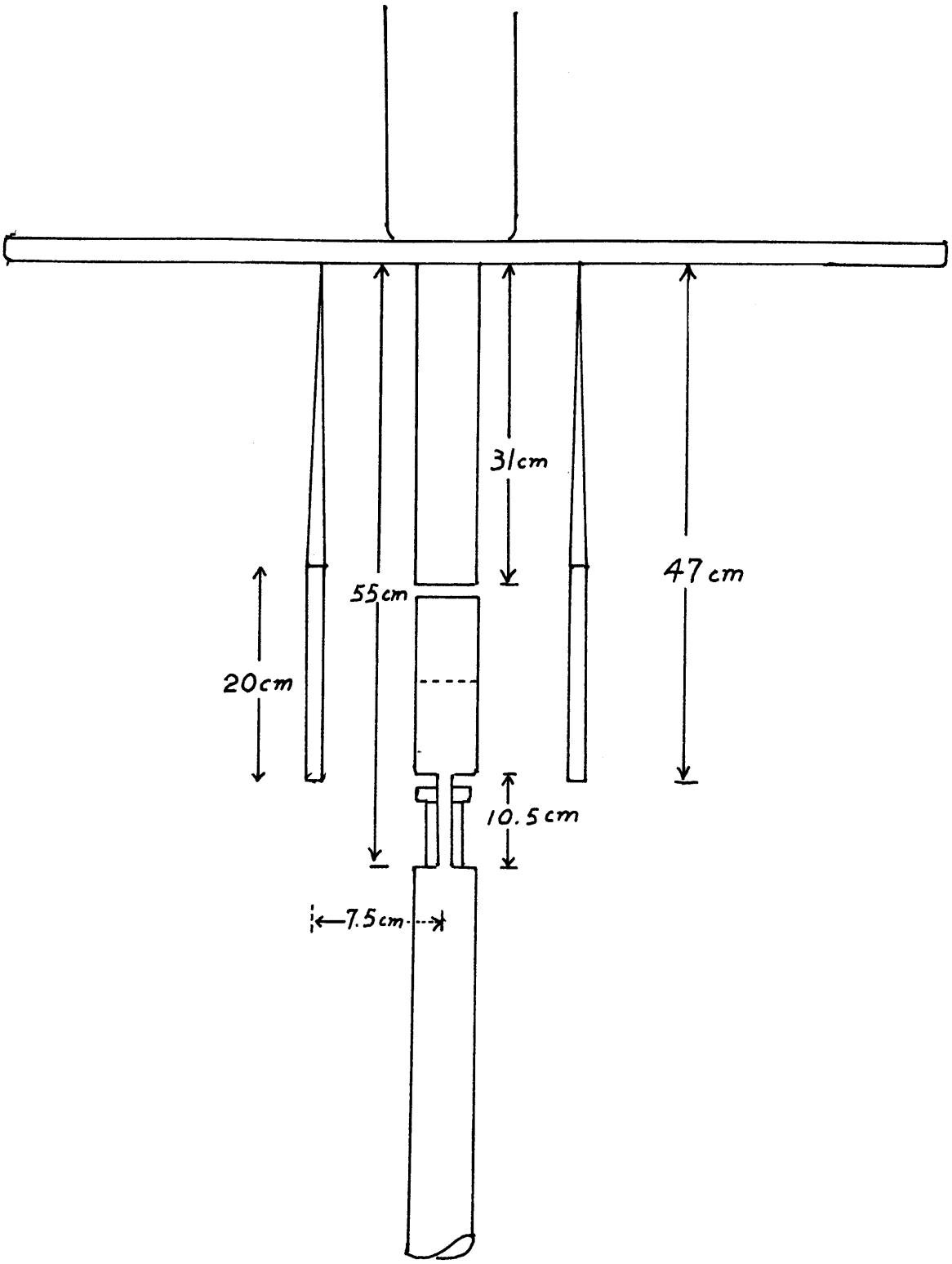

Figure 3.5 Experimental Setup

Element	Sample	Element Weight (gm.)	Run Time (min.)
Lithium	LiCl powder	143	1444
Carbon	Carbon plates	1564	1338
Nitrogen	NH_4NO_3	380	1400
Oxygen	H_2O	958	1262
Magnesium	Mg powder	481	1215
Aluminum	Al plates	3024	1440
Sodium	NaCl	615	1400
Silicon	Glass plates	818	1285
Sulphur	powder	636	1426
Chlorine	NaCl	945	1400
Potassium	KCl powder	658	2089
Titanium	Ti sponge	1016	1440
Vanadium	V scrap	966	1151
Chromium	Cr_2O_3	798	1259
Manganese	Mn pellet	2458	1482
Iron	plates	8184	1339
Cobalt	Co pellet	3808	1026
Nickle	Ni balls	1895	1188
Copper	plates	5863	1059
Lead	plates	11618	1310

Table 3.1 A Table of Sample Type, Run Time and Weight

necessary when filling the scrap sample, owing to their irregular shapes and size, tapping would only give rise to segregation. Then they were weighed (the weight of the aluminum cans were known). Next the samples were put in place as shown in Figure 3.4. The fast neutron source was put in place and the run begun. The analyzer was normally set to run at 2 KEV per channel. The total run time was between 12 to 24 hours with about 4% dead time losses. Before and after each run, the system was calibrated using a Co^{60} source. Every month a background run was made with only the fast neutron source but no sample. A summary of sample type, run times and weight is given in Table 3.1.

All measurements were made inside a cement vault with concrete wall, and ceiling about three feet thick. This provided shielding for the source and also reduced any extraneous background.

Chapter IV

DATA ANALYSIS AND RESULTS

4.1 GAMANL Output

The data obtained from the sample runs was analyzed using the computer code GAMANL. GAMANL is a code developed in this laboratory and described in detail in ref. 4 . Basically the code smooths the data using a Fourier transform method and then calculates peak energies and peak areas.

An example of the final output of GAMANL for a typical run is shown in Table 4.1. The first column is the peak number. The second column is the peak energy measured in KEV. The third column is the peak center channel number. The fourth column is the peak height measured in counts/ channel. The fifth column is the height to background ratio. The sixth column is the area of the peak using both summation method and Gaussian method (to be explained later). The seventh column is the error of the area by both methods. The eighth is a normalized intensity of gamma rays used in earlier work which has no physical significance in these experiments. The full-width-half-maximum of the peak is presented in column nine. The column is the intrinsic efficiency of the detector. The eleventh column is the number of channels wide the peak is at its base. The last

Table 4.1 Sample GAMANL Output

PEAK ANALYSIS PAGE 4

NO	ENERGY KEV	PK CNT CH NO	HEIGHT COUNTS	H TO B RATIO	AREA-S AREA-G COUNTS	ERR-S ERR-G PCSD	INT-S INT-G N/100C	FWHM-M FWHM-C KEV	EFF(E) N/CTS	BASE CHAN	TYPE
47	1099.3	650.4	3347.8	0.2085	19937.5	3.0	0.760	10.69	0.10E-01	14.	S *
					21155.5	4.1	0.806	10.92			
48	1163.0	686.8	1791.6	0.1231	8267.4	5.9	0.336	7.24	0.98E-02	12.	S *
					11334.9	6.1	0.460	10.93			
49	1191.1	702.8	9082.8	0.6345	57985.6	1.1	2.422	11.18	0.96E-02	16.	S *
					57481.6	3.4	2.401	10.93			
50	1265.9	745.0	524.2	0.0460	2653.1	11.8	0.119	9.44	0.89E-02	8.	S *
					3318.6	15.5	0.149	10.94			
51	1293.6	760.7	2077.1	0.1946	13378.4	4.0	0.618	10.95	0.87E-02	16.	S *
					13148.4	5.6	0.607	10.94			
52	1392.6	817.6	323.3	0.0359	1701.2	19.4	0.086	9.94	0.79E-02	10.	S *
					2044.4	21.9	0.104	10.92			
53	1430.3	839.0	931.3	0.1069	4264.4	7.7	0.223	8.08	0.76E-02	10.	S *
					5883.9	9.1	0.308	10.92			
54	1460.3	856.2	4423.4	0.5083	32729.6	1.6	1.759	12.56	0.74E-02	16.	S *
					27926.2	5.4	1.501	10.91			
55	1483.0	869.4	1916.3	0.2307	13217.6	3.4	0.724	12.00	0.73E-02	15.	S *
					12090.3	6.5	0.662	10.90			
56	1588.3	929.6	283.6	0.0418	1616.2	15.3	0.093	10.85	0.69E-02	12.	D .524
					1781.8	22.2	0.103	10.85			
57	1594.0	932.9	170.0	0.0251	1020.2	15.3	0.059	10.85	0.69E-02	12.	D .524
					1068.1	35.6	0.062	10.85			
58	1745.4	1019.1	808.9	0.1361	5350.5	6.3	0.332	12.25	0.64E-02	13.	S *
					5037.2	10.7	0.313	10.76			
59	1779.5	1038.6	246.2	0.0421	957.1	23.3	0.060	7.26	0.63E-02	8.	S *
					1529.3	24.2	0.097	10.73			
60	2089.0	1216.0	258.8	0.0635	1204.3	17.0	0.089	8.24	0.54E-02	9.	S *
					1560.2	22.8	0.115	10.42			
61	2203.7	1282.2	437.3	0.1222	3547.7	9.4	0.277	10.26	0.51E-02	24.	D .276
					2596.3	19.9	0.203	10.26			
62	2210.0	1285.9	285.0	0.0796	2341.2	9.4	0.183	10.26	0.51E-02	24.	D .276
					1692.3	23.1	0.133	10.26			

column shows whether the peak is a singlet(S) or a doublet (D) or a triplet (T). A star sign (*) besides the singlet symbol (S) means it is a "strong" singlet.

After subtracting the background, the area under each peak was proportional to the intensity(counts/min x gm) of that gamma energy. The area was determined by two methods. First, the summation method which simply sums up the counts of each channel which are inside the peak. Second, the Gaussian method, which assumes each peak is approximately Gaussian shape, thus knowing the height of the peak (from experimental data) and the standard deviation(determined theoratically, ref. 5), the area can be calculated. The result of the summation method is always used unless the peak is part of multiplets, then the Gaussian method is used because experience has shown it to be somewhat more accurate in this case. The error of both methods is discussed in detail by Hamawi (ref. 5) and Harper(ref. 6). It is sufficient to say here that the error depends mainly on the accuracy of the background determination. Data of every run was plotted by computer and the spectra are shown in Figure 4.1 to Figure 4.18.

4.2 Identification of Gamma Lines

From the background run, all the strong background lines were identified and they are shown in Table 4.2.

If a gamma ray is higher than 1.022 MEV, then it is

Table 4.2

Table of Strong Background Lines

Element	Energy KEV (±5KEV)	Intensity (counts / min x gm)	Error
Pb	539	2.98	17%
Ge, Pb	562	11.58	6%
Ge	595	51.15	2%
Cu cap	606	22.81	3%
Pb	669	6.83	6%
Ge	696	163.59	2%
Pb	797	2.42	17%
Pb	804	3.10	13%
Ge	835	15.47	3%
Al,Fe	844	11.42	4%
Pb	870	3.18	10%
Pb	901	2.04	18%
Cu	963	9.37	4%
Al	1015	6.75	5%
Cu	1117	4.42	7%
H cap (DE)	1203	2.87	10%
Si	1274	1.23	23%
Cu	1327	3.52	7%
Fe	1414	1.93	13%
Pb	1462	7.98	4%
Pb (DE)	1592	3.81	6%

cap ----- capture gamma

(DE) ------ Double Escape peak

Table 4.2 (Contd.)

Element	Energy KEV (± 5KEV)	Intensity $\left(\frac{\text{counts}}{\text{min x gm}}\right)$	Error
Cl	1762	0.90	23%
Si, Al cap	1778	4.66	5%
Al	1993	0.63	21%
H cap	2223	1.45	12%
N	2303	0.26	27%
Si cap (DE)	2517	1.03	14%
Pb	2614	2.56	7%
Si cap (DE)	3912	1.34	8%
O (DE)	5108	1.34	7%
Ca cap (DE)	5398	0.58	15%
Cu cap (DE)	6285	0.19	20%
Fe cap (DE)	6615	1.06	10%
Cu cap (DE)	6893	0.67	9%

cap ---- capture gamma

(DE) ---- Double Escape peak

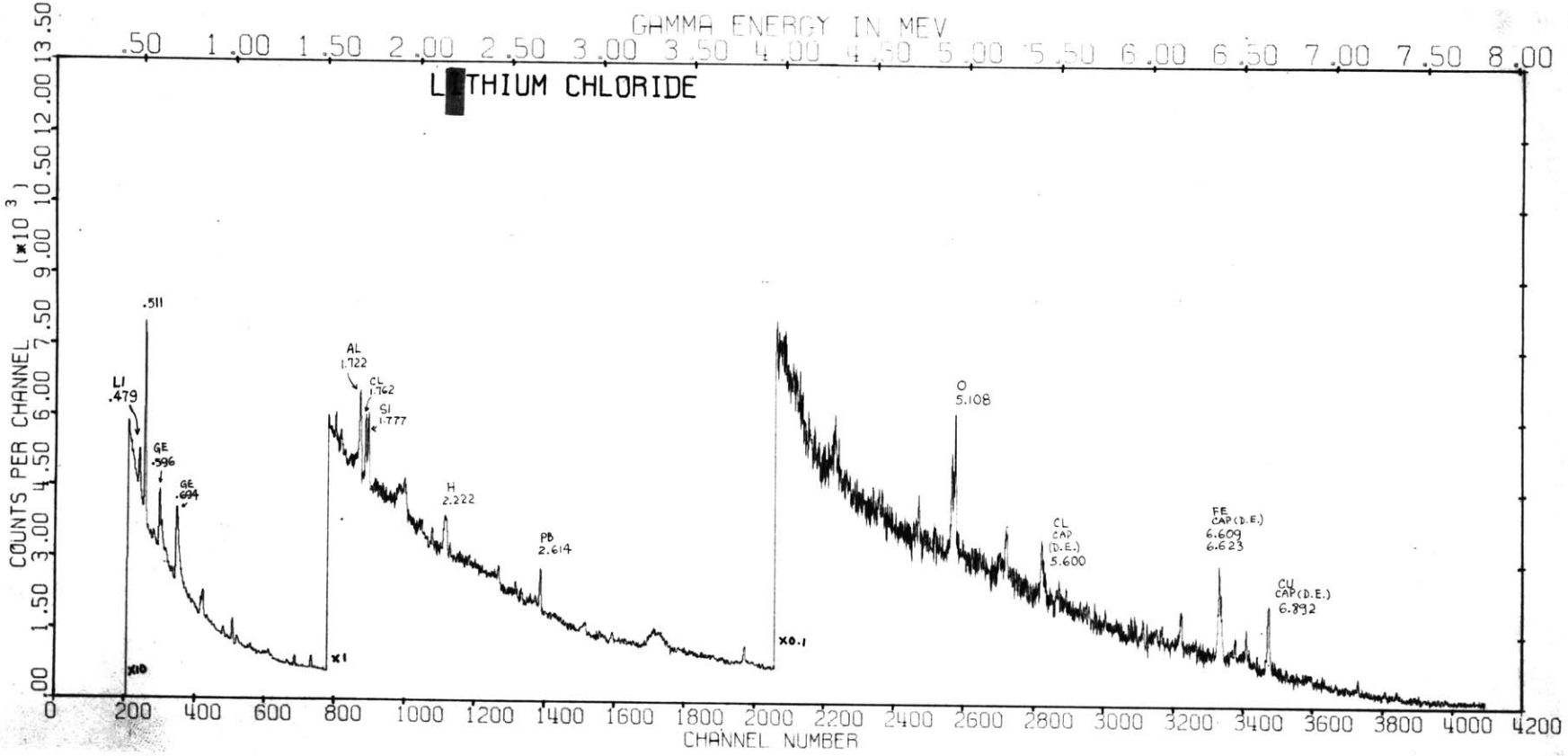
GAMMA ENERGY IN MEV
.50 1.00 1.50 2.00 2.50 3.00 3.50 4.00 4.50 5.00 5.50 6.00 6.50 7.00 7.50 8.00
LITHIUM CHLORIDE
COUNTS PER CHANNEL (*10^3)
.00 1.50 3.00 4.50 6.00 7.50 9.00 10.50 12.00 13.50
.511
LI .479
GE .596
GE .694
AL 1.722
CL 1.762
SI 1.777
H 2.222
PB 2.614
O 5.108
CL CAP (D.E.) 5.600
FE CAP(D.E.) 6.609 6.623
CU CAP(D.E.) 6.892
x10
x1
x0.1
0 200 400 600 800 1000 1200 1400 1600 1800 2000 2200 2400 2600 2800 3000 3200 3400 3600 3800 4000 4200
CHANNEL NUMBER

Figure 4.1

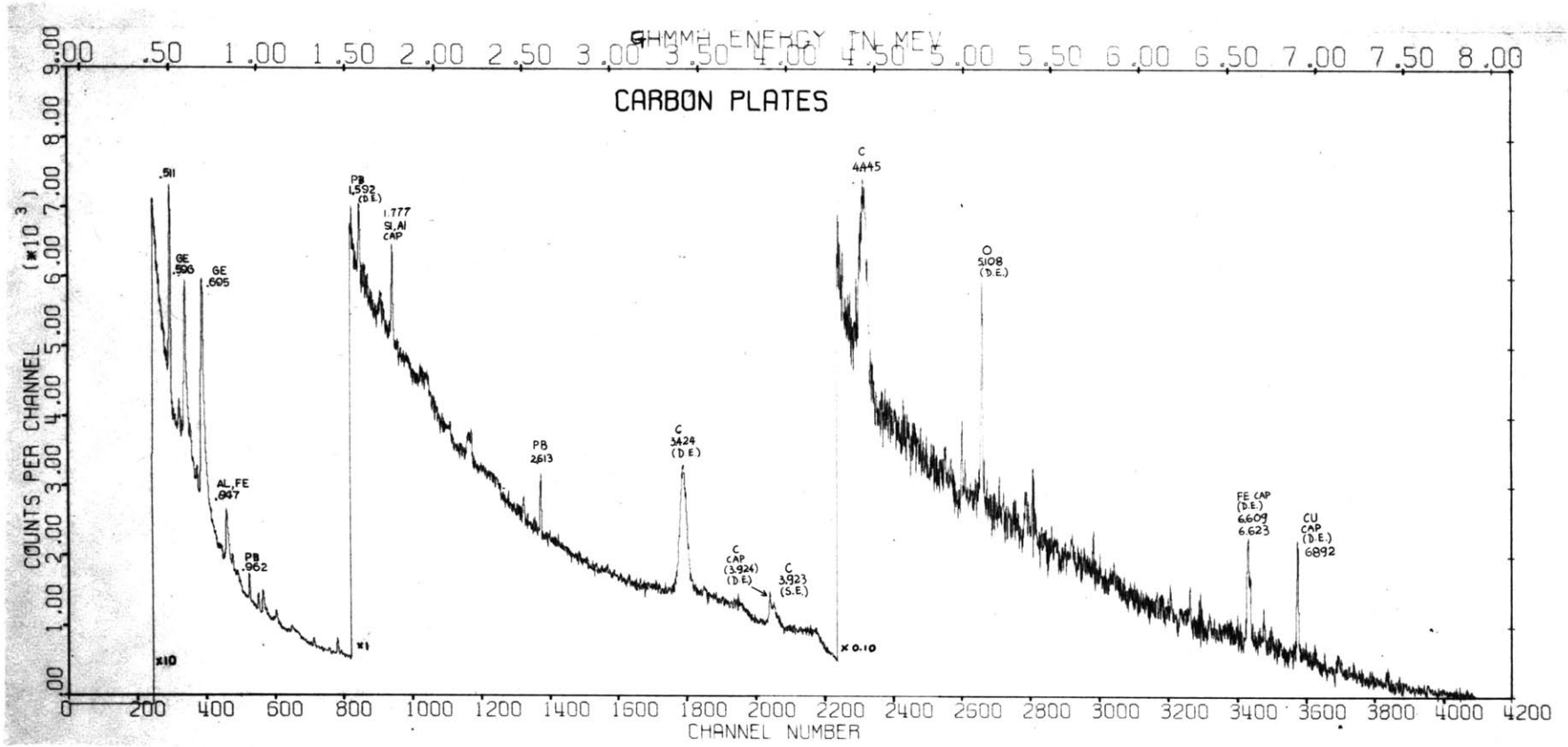
GAMMA ENERGY IN MEV
.50 1.00 1.50 2.00 2.50 3.00 3.50 4.00 4.50 5.00 5.50 6.00 6.50 7.00 7.50 8.00
CARBON PLATES
COUNTS PER CHANNEL (*10^3)
.00 1.00 2.00 3.00 4.00 5.00 6.00 7.00 8.00 9.00
.511
GE .596
GE .605
AL,FE .847
PB .962
PB 1.592 (D.E.)
1.777 SI,AI CAP
PB 2.613
C 3.424 (D.E.)
C CAP (3.924) (D.E.)
C 3.923 (S.E.)
C 4.445
O 5.108 (D.E.)
FE CAP (D.E.) 6.609 6.623
CU CAP (D.E.) 6.892
x10
x1
x 0.10
0 200 400 600 800 1000 1200 1400 1600 1800 2000 2200 2400 2600 2800 3000 3200 3400 3600 3800 4000 4200
CHANNEL NUMBER

Figure 4.2

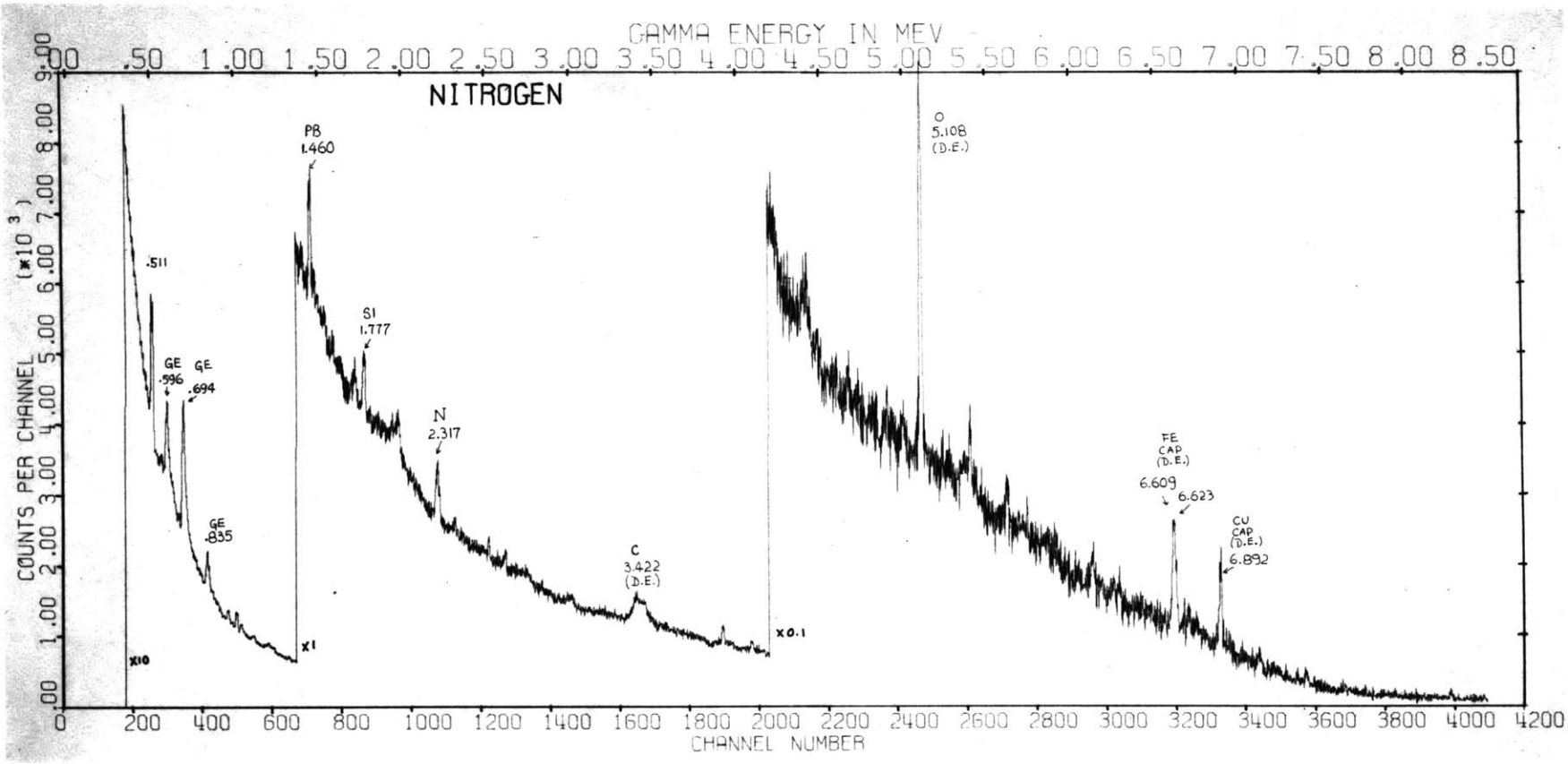
GAMMA ENERGY IN MEV
.00 .50 1.00 1.50 2.00 2.50 3.00 3.50 4.00 4.50 5.00 5.50 6.00 6.50 7.00 7.50 8.00 8.50
NITROGEN
COUNTS PER CHANNEL (*10 3)
.00 1.00 2.00 3.00 4.00 5.00 6.00 7.00 8.00 9.00
.511
GE .596
GE .694
GE .835
PB 1.460
SI 1.777
N 2.317
C 3.422 (D.E.)
O 5.108 (D.E.)
FE CAP (D.E.) 6.609
6.623
CU CAP (D.E.) 6.892
X10
X1
X0.1
0 200 400 600 800 1000 1200 1400 1600 1800 2000 2200 2400 2600 2800 3000 3200 3400 3600 3800 4000 4200
CHANNEL NUMBER

Figure 4.3

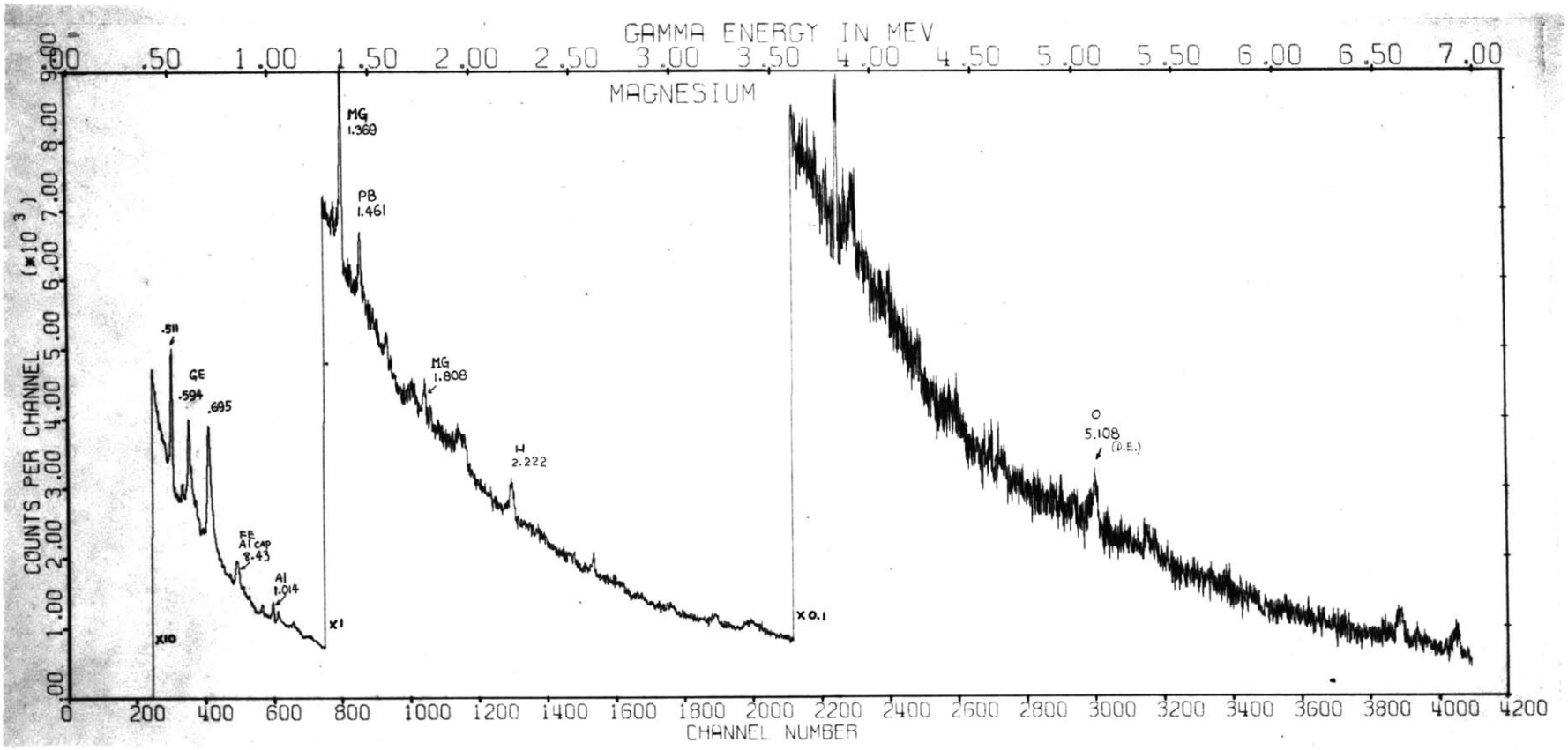
GAMMA ENERGY IN MEV
.50 1.00 1.50 2.00 2.50 3.00 3.50 4.00 4.50 5.00 5.50 6.00 6.50 7.00
MAGNESIUM
COUNTS PER CHANNEL (*10^3)
.00 1.00 2.00 3.00 4.00 5.00 6.00 7.00 8.00 9.00
MG 1.369
PB 1.461
MG 1.808
H 2.222
O 5.108 (D.E.)
.511
GE .594
.695
FE Al cap 8.43
Al 1.014
X10
X1
X0.1
0 200 400 600 800 1000 1200 1400 1600 1800 2000 2200 2400 2600 2800 3000 3200 3400 3600 3800 4000 4200
CHANNEL NUMBER

Figure 4.4

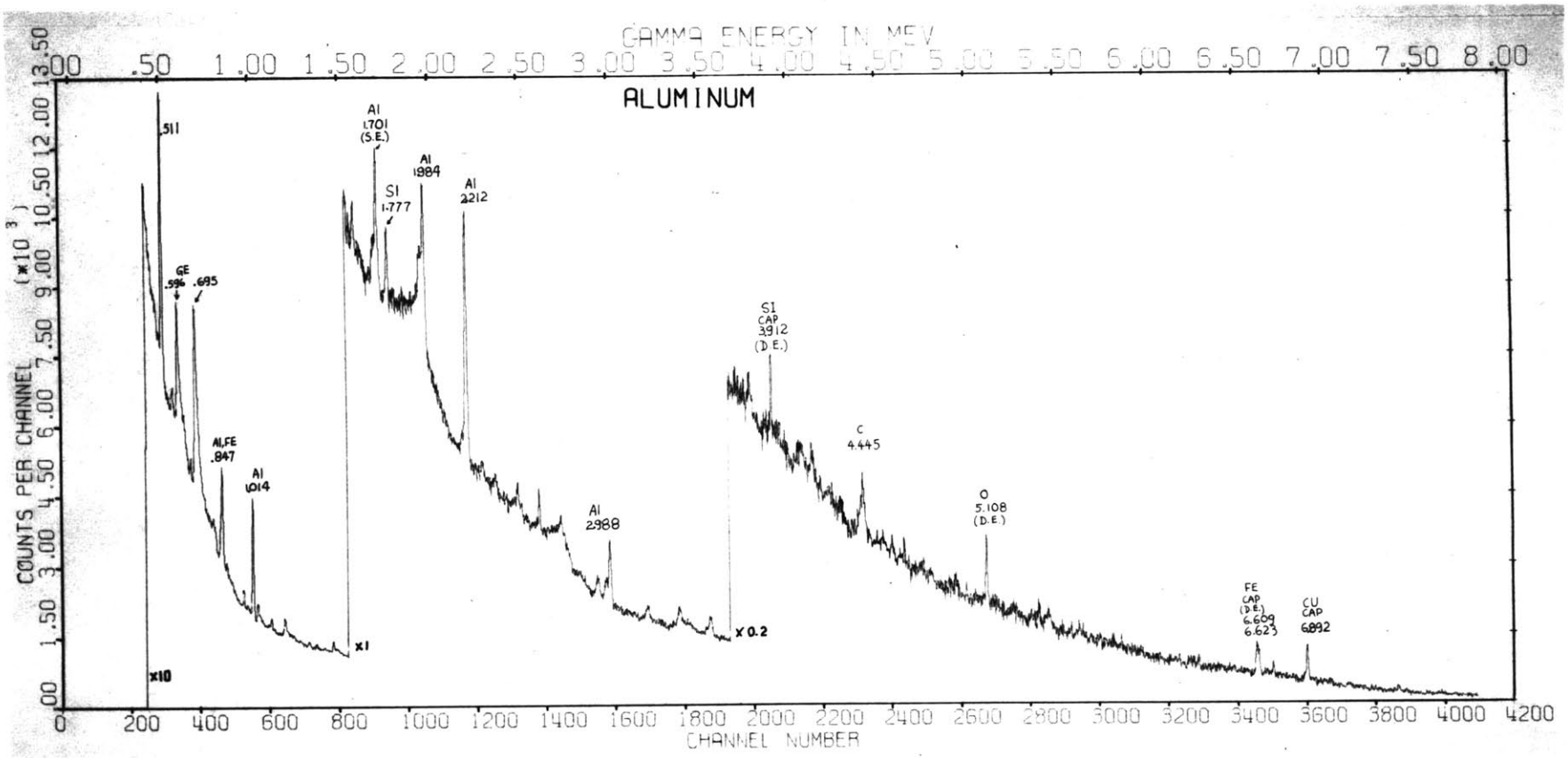
GAMMA ENERGY IN MEV
.00 .50 1.00 1.50 2.00 2.50 3.00 3.50 4.00 4.50 5.00 5.50 6.00 6.50 7.00 7.50 8.00
ALUMINUM
COUNTS PER CHANNEL (*10^3)
.00 1.50 3.00 4.50 6.00 7.50 9.00 10.50 12.00 13.50
.511
GE .596
.695
AL,FE .847
AL 1014
AL 1701 (S.E.)
SI 1.777
AL 1984
AL 2212
AL 2988
SI CAP 3.912 (D.E.)
C 4.445
O 5.108 (D.E.)
FE CAP (D.E.) 6.609 6.623
CU CAP 6.892
x10
x1
x0.2
0 200 400 600 800 1000 1200 1400 1600 1800 2000 2200 2400 2600 2800 3000 3200 3400 3600 3800 4000 4200
CHANNEL NUMBER

Figure 4.5

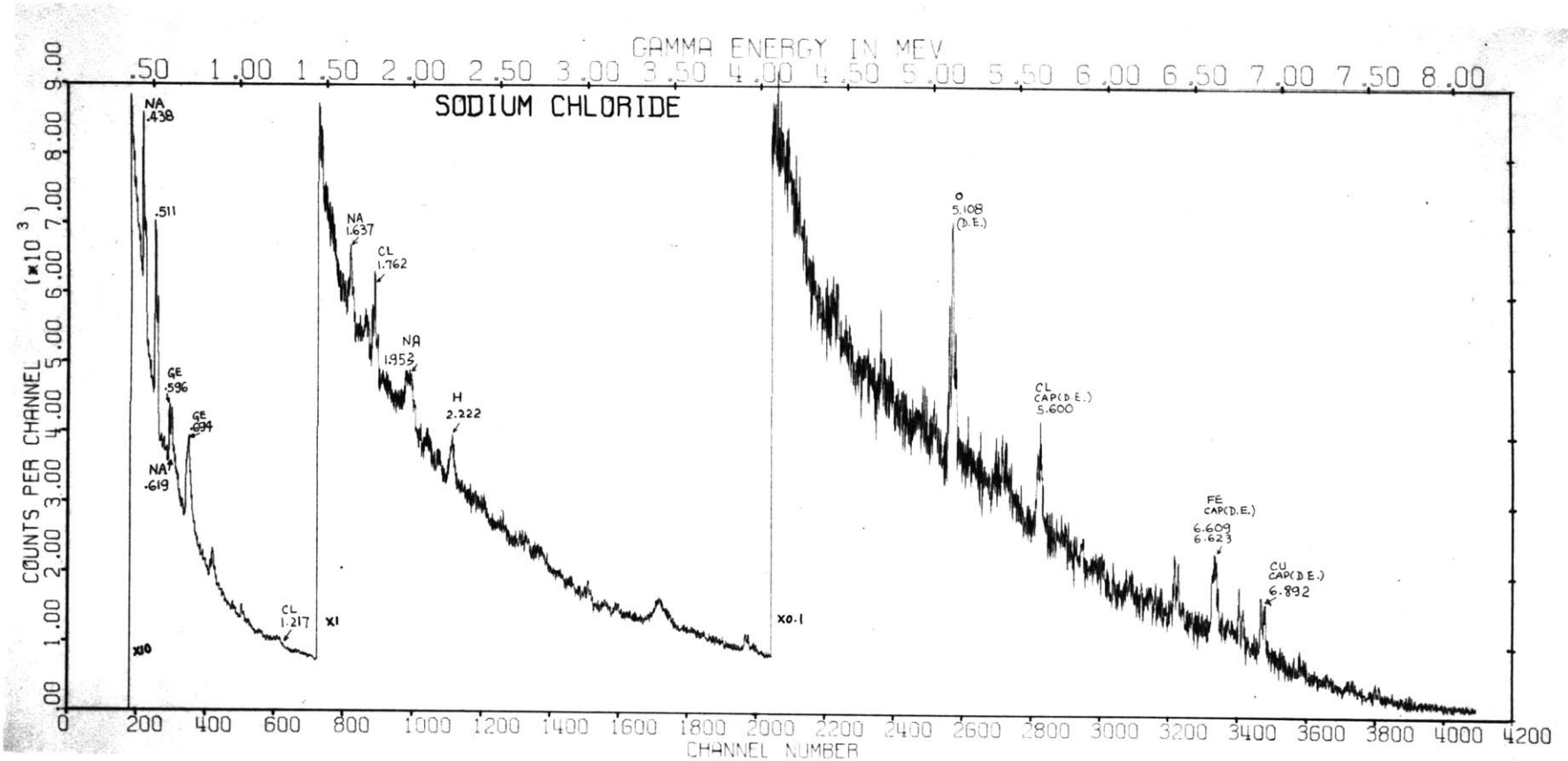
SODIUM CHLORIDE
GAMMA ENERGY IN MEV
.50 1.00 1.50 2.00 2.50 3.00 3.50 4.00 4.50 5.00 5.50 6.00 6.50 7.00 7.50 8.00
COUNTS PER CHANNEL (×10 3)
.00 1.00 2.00 3.00 4.00 5.00 6.00 7.00 8.00 9.00
NA .438
.511
GE .596
GE .694
NA .619
CL 1.217
X10
X1
NA 1.637
CL 1.762
NA 1.953
H 2.222
X0.1
O 5.108 (D.E.)
CL CAP(D.E.) 5.600
FE CAP(D.E.) 6.609 6.623
CU CAP(D.E.) 6.892
0 200 400 600 800 1000 1200 1400 1600 1800 2000 2200 2400 2600 2800 3000 3200 3400 3600 3800 4000 4200
CHANNEL NUMBER

Figure 4.6

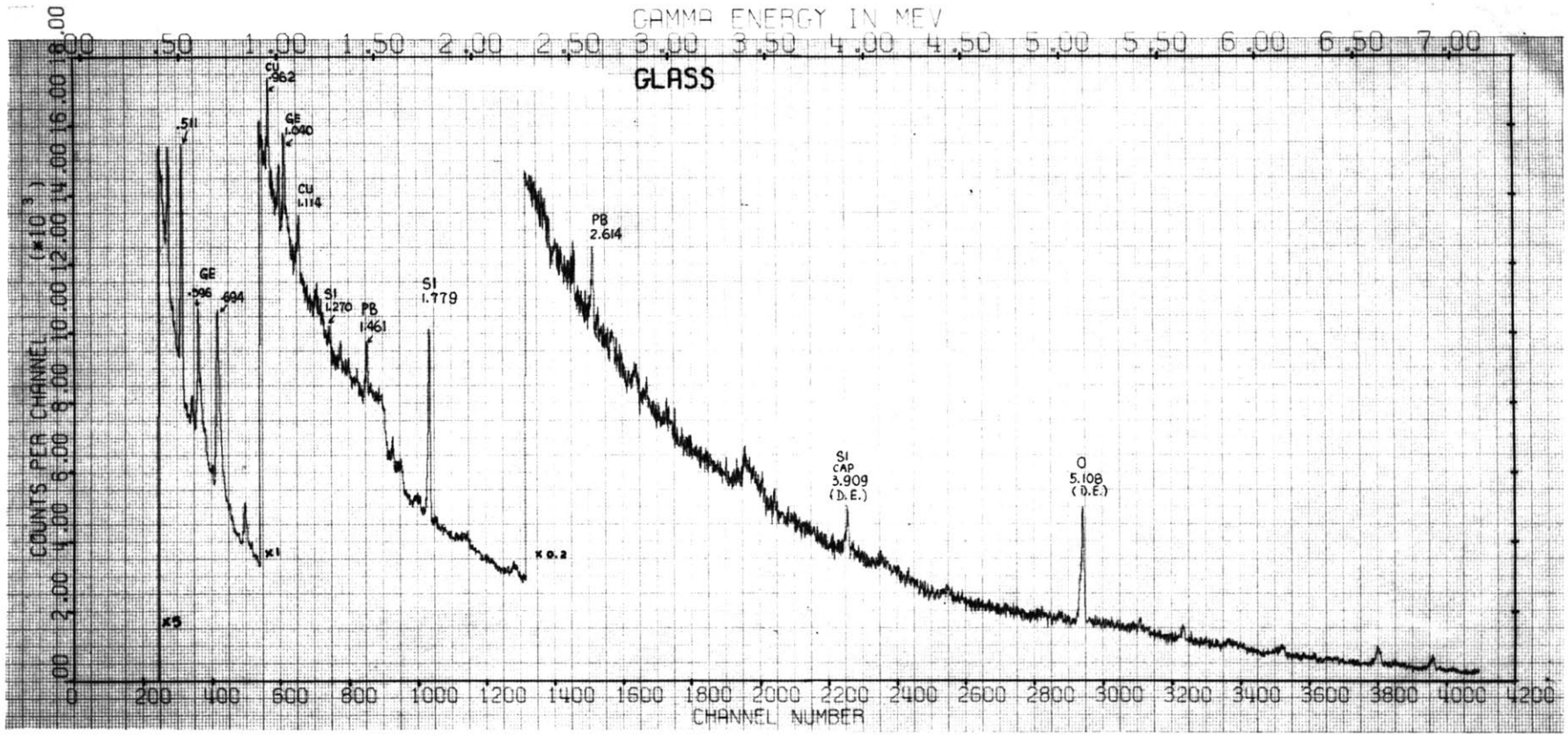
GAMMA ENERGY IN MEV
.50 1.00 1.50 2.00 2.50 3.00 3.50 4.00 4.50 5.00 5.50 6.00 6.50 7.00
GLASS
COUNTS PER CHANNEL (*10³)
.00 2.00 4.00 6.00 8.00 10.00 12.00 14.00 16.00 18.00
CU .962
GE 1.040
.511
CU 1.114
GE .596
.694
SI 1.270
PB 1.461
SI 1.779
PB 2.614
SI CAP 3.909 (D.E.)
O 5.108 (D.E.)
x1
x0.2
x5
0 200 400 600 800 1000 1200 1400 1600 1800 2000 2200 2400 2600 2800 3000 3200 3400 3600 3800 4000 4200
CHANNEL NUMBER

Figure 4.7

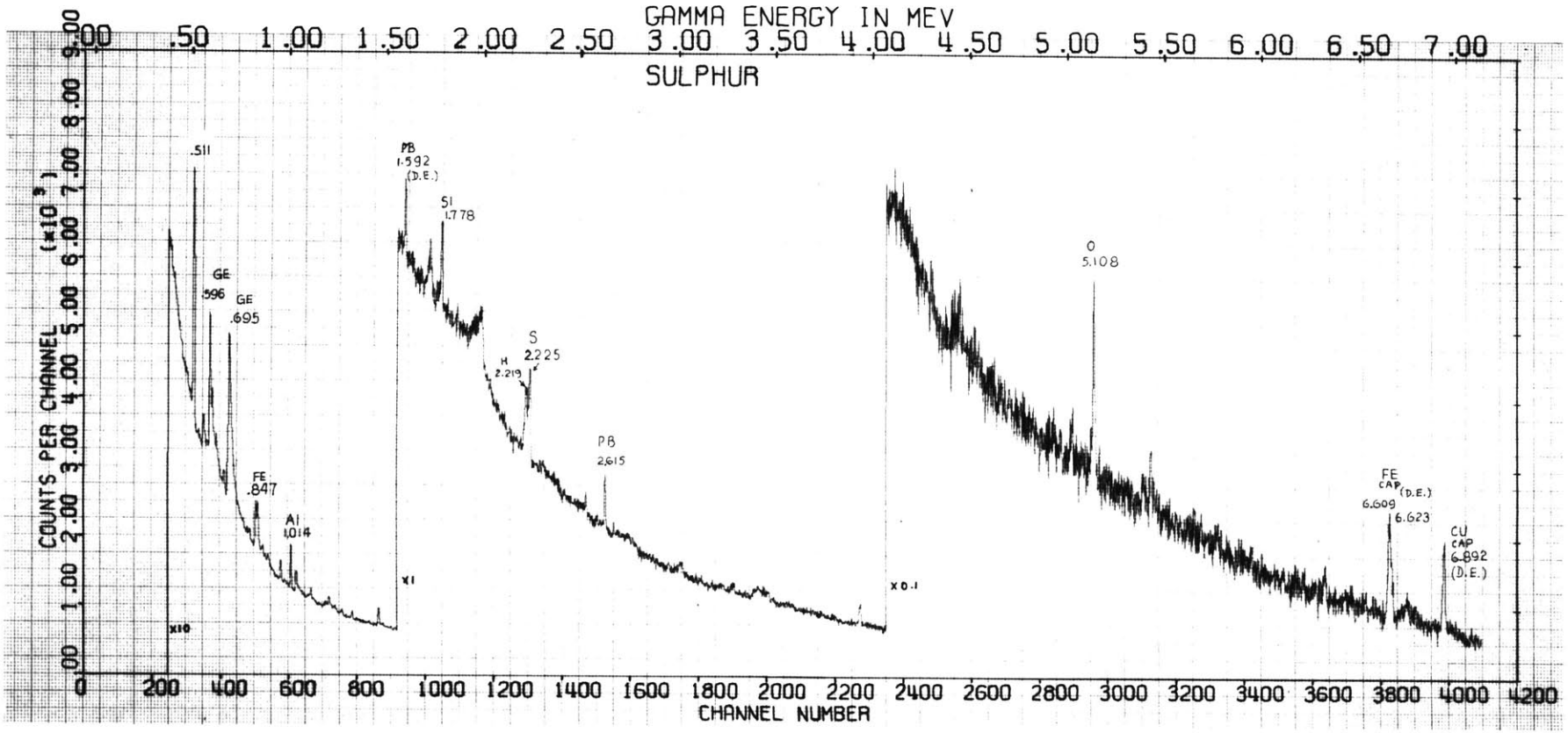
GAMMA ENERGY IN MEV
.50 1.00 1.50 2.00 2.50 3.00 3.50 4.00 4.50 5.00 5.50 6.00 6.50 7.00
SULPHUR
COUNTS PER CHANNEL (×10³)
0.00 1.00 2.00 3.00 4.00 5.00 6.00 7.00 8.00 9.00
.511
GE .596
GE .695
FE .847
Al 1.014
PB 1.592 (D.E.)
SI 1.778
H 2.219
S 2.225
PB 2.615
O 5.108
FE CAP (D.E.) 6.609
6.623
CU CAP 6.892 (D.E.)
x10
x1
x0.1
0 200 400 600 800 1000 1200 1400 1600 1800 2000 2200 2400 2600 2800 3000 3200 3400 3600 3800 4000 4200
CHANNEL NUMBER

Figure 4.8

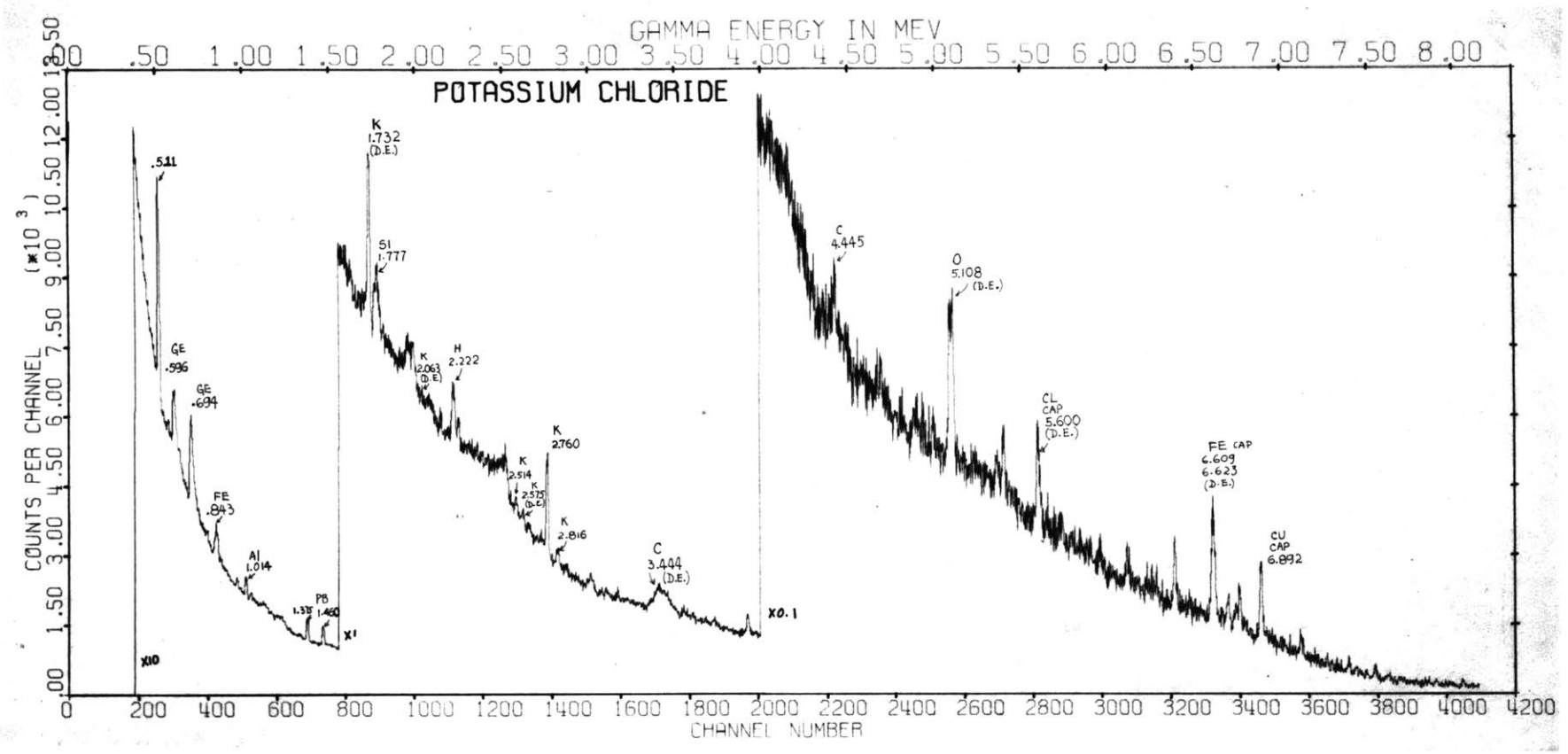
POTASSIUM CHLORIDE
GAMMA ENERGY IN MEV
.50 1.00 1.50 2.00 2.50 3.00 3.50 4.00 4.50 5.00 5.50 6.00 6.50 7.00 7.50 8.00
COUNTS PER CHANNEL (*10 3)
.00 1.50 3.00 4.50 6.00 7.50 9.00 10.50 12.00 13.50
CHANNEL NUMBER
0 200 400 600 800 1000 1200 1400 1600 1800 2000 2200 2400 2600 2800 3000 3200 3400 3600 3800 4000 4200
.511
GE .596
GE .694
FE .843
AL 1.014
PB 1.460
K 1.732 (D.E.)
SI 1.777
K 2.063 (D.E.)
H 2.222
K 2.514
K 2.535 (D.E.)
K 2.760
K 2.816
C 3.444 (D.E.)
C 4.445
O 5.108 (D.E.)
CL CAP 5.600 (D.E.)
FE CAP 6.609 6.623 (D.E.)
CU CAP 6.892
X10
X1
X0.1

Figure 4.9

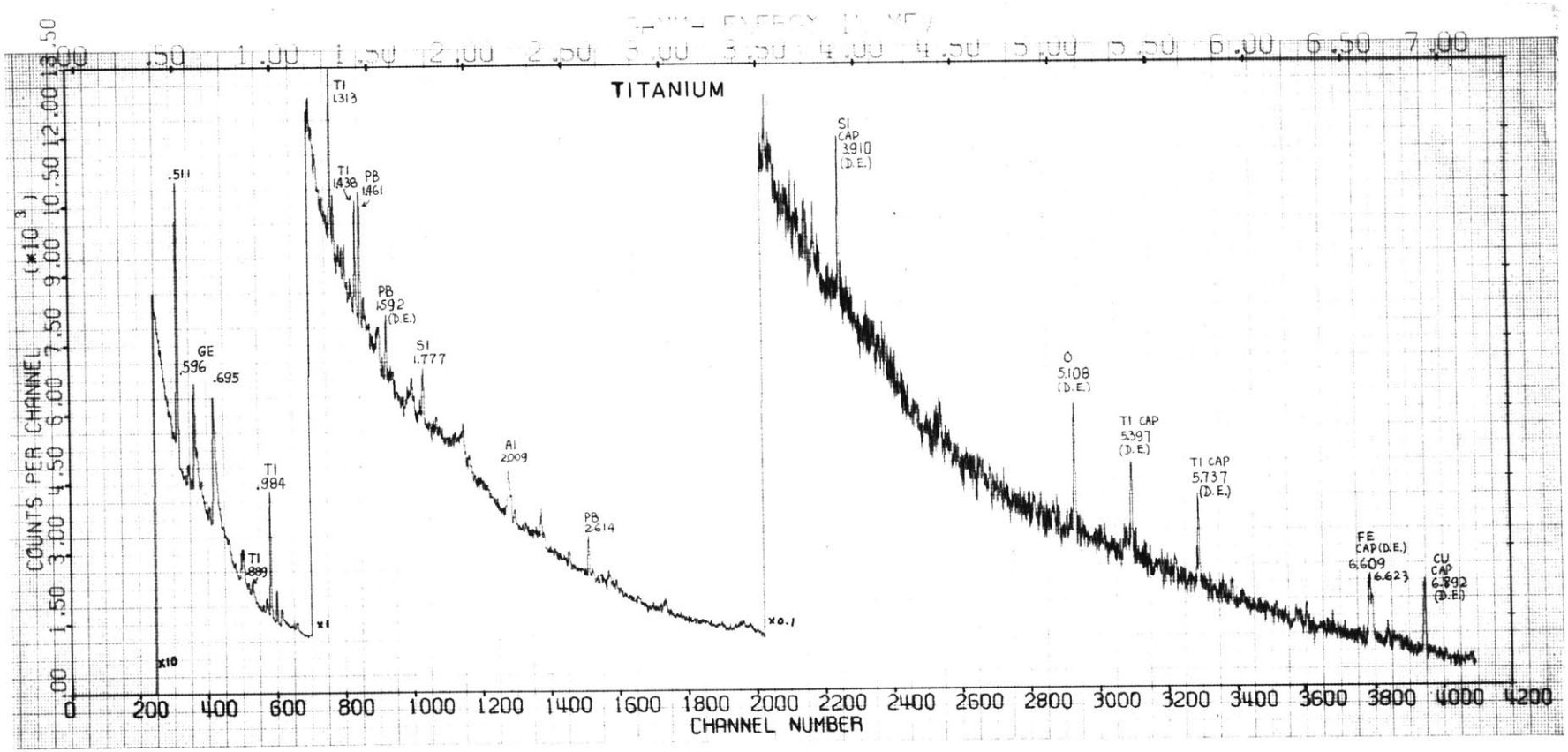
TITANIUM
COUNTS PER CHANNEL (*10^3)
CHANNEL NUMBER
.511
GE .596
.695
TI .984
TI .889
TI 1.313
TI 1.438
PB 1.461
PB 1.592 (D.E.)
SI 1.777
AL 2.009
PB 2.614
SI CAP 3.910 (D.E.)
O 5.108 (D.E.)
TI CAP 5.397 (D.E.)
TI CAP 5.737 (D.E.)
FE CAP (D.E.) 6.609
6.623
CU CAP 6.892 (D.E.)
x10
x1
x0.1

Figure 4.10

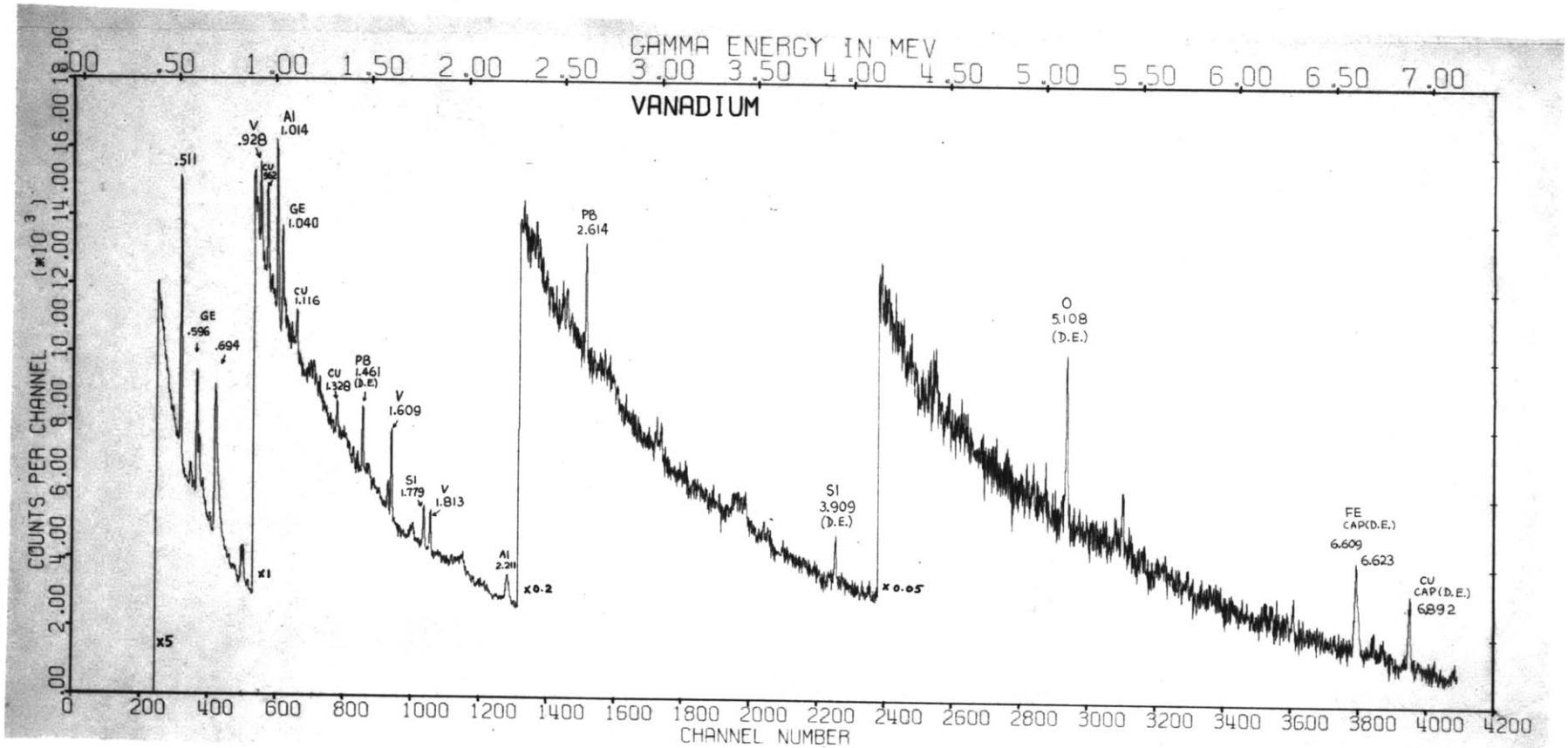
GAMMA ENERGY IN MEV
.00 .50 1.00 1.50 2.00 2.50 3.00 3.50 4.00 4.50 5.00 5.50 6.00 6.50 7.00
VANADIUM
COUNTS PER CHANNEL (*10^3)
.00 2.00 4.00 6.00 8.00 10.00 12.00 14.00 16.00 18.00
.511
V .928
CU .952
AL 1.014
GE 1.040
CU 1.116
GE .596
.694
CU 1.328
PB 1.461 (D.E.)
V 1.609
SI 1.779
V 1.813
AL 2.211
PB 2.614
SI 3.909 (D.E.)
O 5.108 (D.E.)
FE CAP(D.E.) 6.609
6.623
CU CAP(D.E.) 6.892
x5
x1
x0.2
x0.05
0 200 400 600 800 1000 1200 1400 1600 1800 2000 2200 2400 2600 2800 3000 3200 3400 3600 3800 4000 4200
CHANNEL NUMBER

Figure 4.11

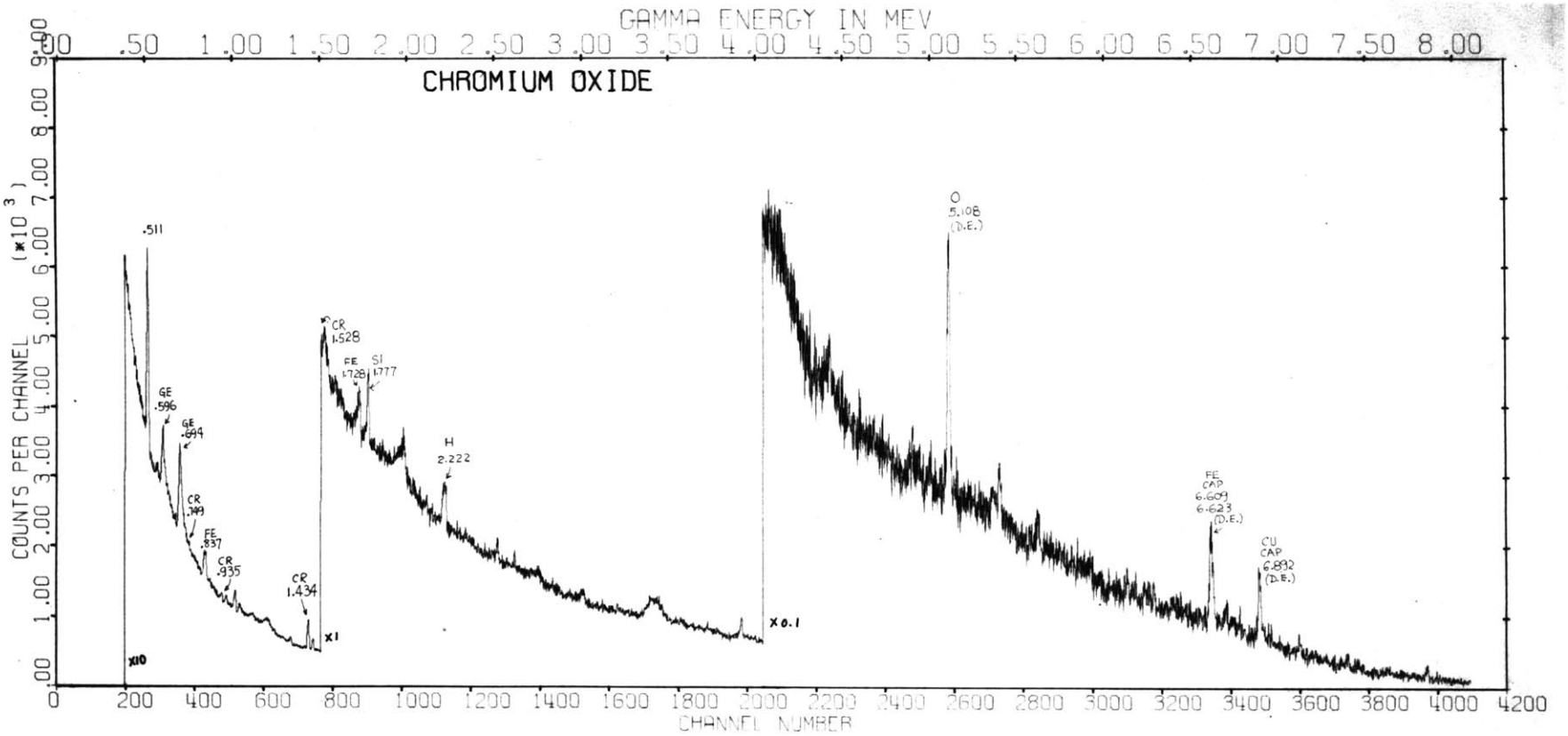
GAMMA ENERGY IN MEV
.00 .50 1.00 1.50 2.00 2.50 3.00 3.50 4.00 4.50 5.00 5.50 6.00 6.50 7.00 7.50 8.00
CHROMIUM OXIDE
COUNTS PER CHANNEL (*10 3)
.00 1.00 2.00 3.00 4.00 5.00 6.00 7.00 8.00 9.00
.511
GE .596
GE .694
CR .749
FE .837
CR .935
CR 1.434
CR 1.528
FE 1.728
SI 1.777
H 2.222
O 5.108 (D.E.)
FE CAP 6.609 6.623 (D.E.)
CU CAP 6.892 (D.E.)
x10
x1
x0.1
0 200 400 600 800 1000 1200 1400 1600 1800 2000 2200 2400 2600 2800 3000 3200 3400 3600 3800 4000 4200
CHANNEL NUMBER

Figure 4.12

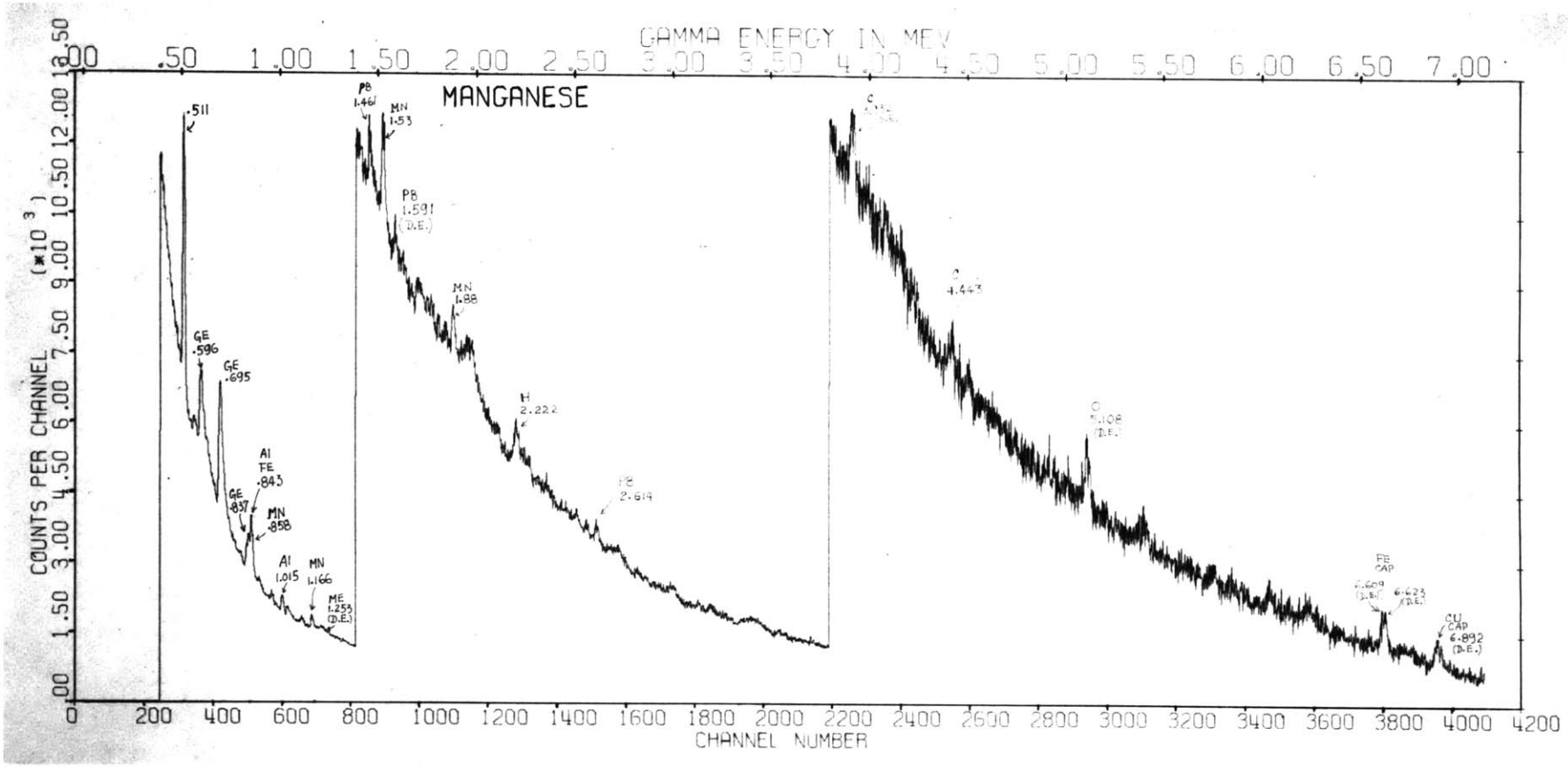
MANGANESE
GAMMA ENERGY IN MEV
.00 .50 1.00 1.50 2.00 2.50 3.00 3.50 4.00 4.50 5.00 5.50 6.00 6.50 7.00
COUNTS PER CHANNEL (*10^3)
.00 1.50 3.00 4.50 6.00 7.50 9.00 10.50 12.00 13.50
0 200 400 600 800 1000 1200 1400 1600 1800 2000 2200 2400 2600 2800 3000 3200 3400 3600 3800 4000 4200
CHANNEL NUMBER
.511
GE .596
GE .695
GE .857
AL FE .843
MN .858
AL 1.015
MN 1.166
ME 1.253 (D.E.)
PB 1.461
MN 1.53
PB 1.591 (D.E.)
MN 1.88
H 2.222
FE 2.619
C 4.443
O 5.108 (D.E.)
FE ESC
6.623 (D.E.)
CU CAP 6.892 (D.E.)

Figure 4.13

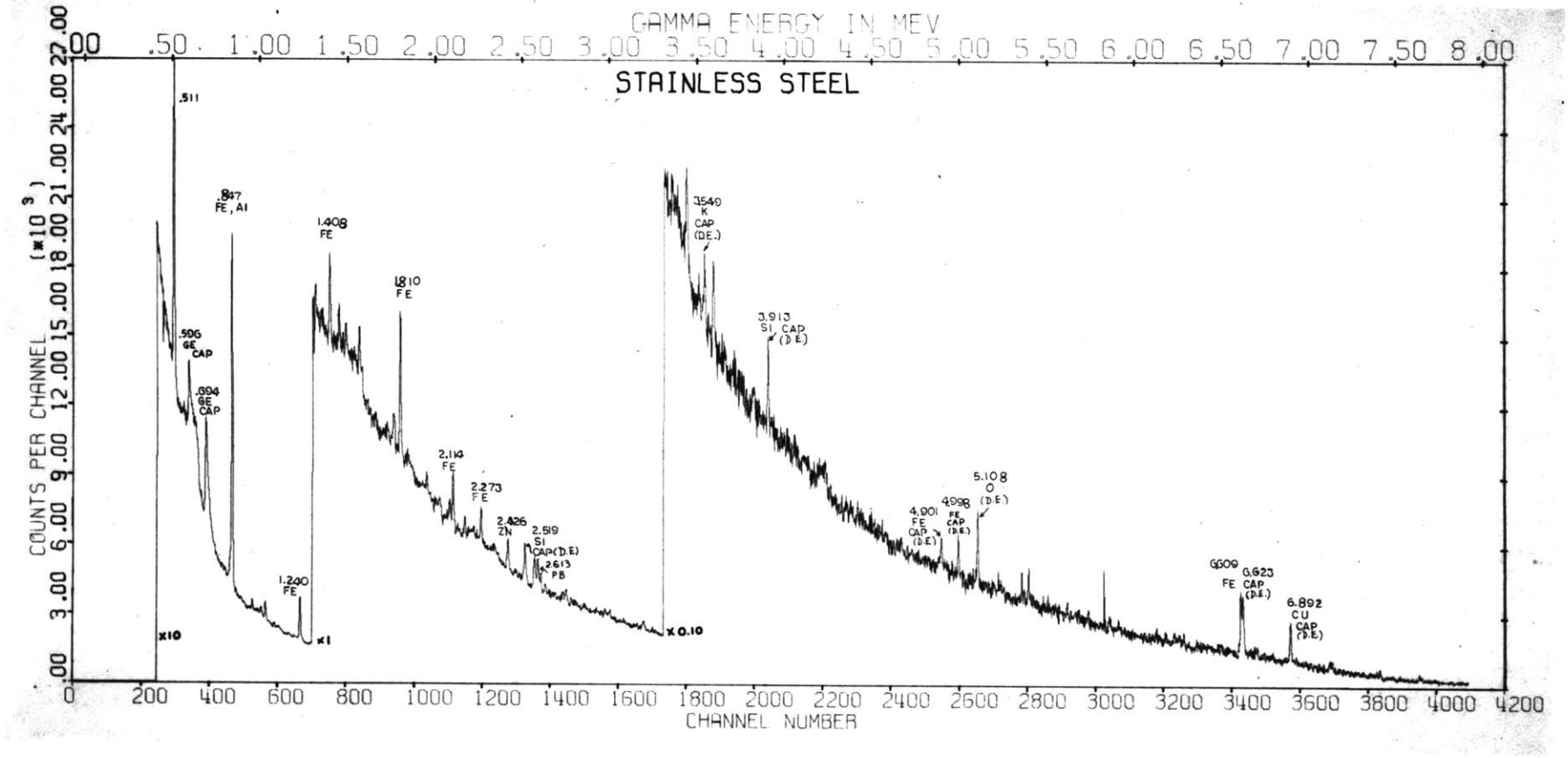
GAMMA ENERGY IN MEV
.50 1.00 1.50 2.00 2.50 3.00 3.50 4.00 4.50 5.00 5.50 6.00 6.50 7.00 7.50 8.00
STAINLESS STEEL
COUNTS PER CHANNEL (*10 3)
.00 3.00 6.00 9.00 12.00 15.00 18.00 21.00 24.00 22.00
.511
.847 FE, AI
1.408 FE
1.810 FE
.506 GE CAP
.694 GE CAP
1.240 FE
2.114 FE
2.273 FE
2.426 ZN
2.519 SI CAP(D.E)
2.613 PB
3.549 K CAP (D.E.)
3.913 SI CAP (D.E)
4.901 FE CAP (D.E.)
4.998 FE CAP (D.E.)
5.108 O (D.E.)
6.609 FE
6.623 CAP (D.E.)
6.892 CU CAP (D.E.)
x10
x1
x 0.10
0 200 400 600 800 1000 1200 1400 1600 1800 2000 2200 2400 2600 2800 3000 3200 3400 3600 3800 4000 4200
CHANNEL NUMBER

Figure 4.14

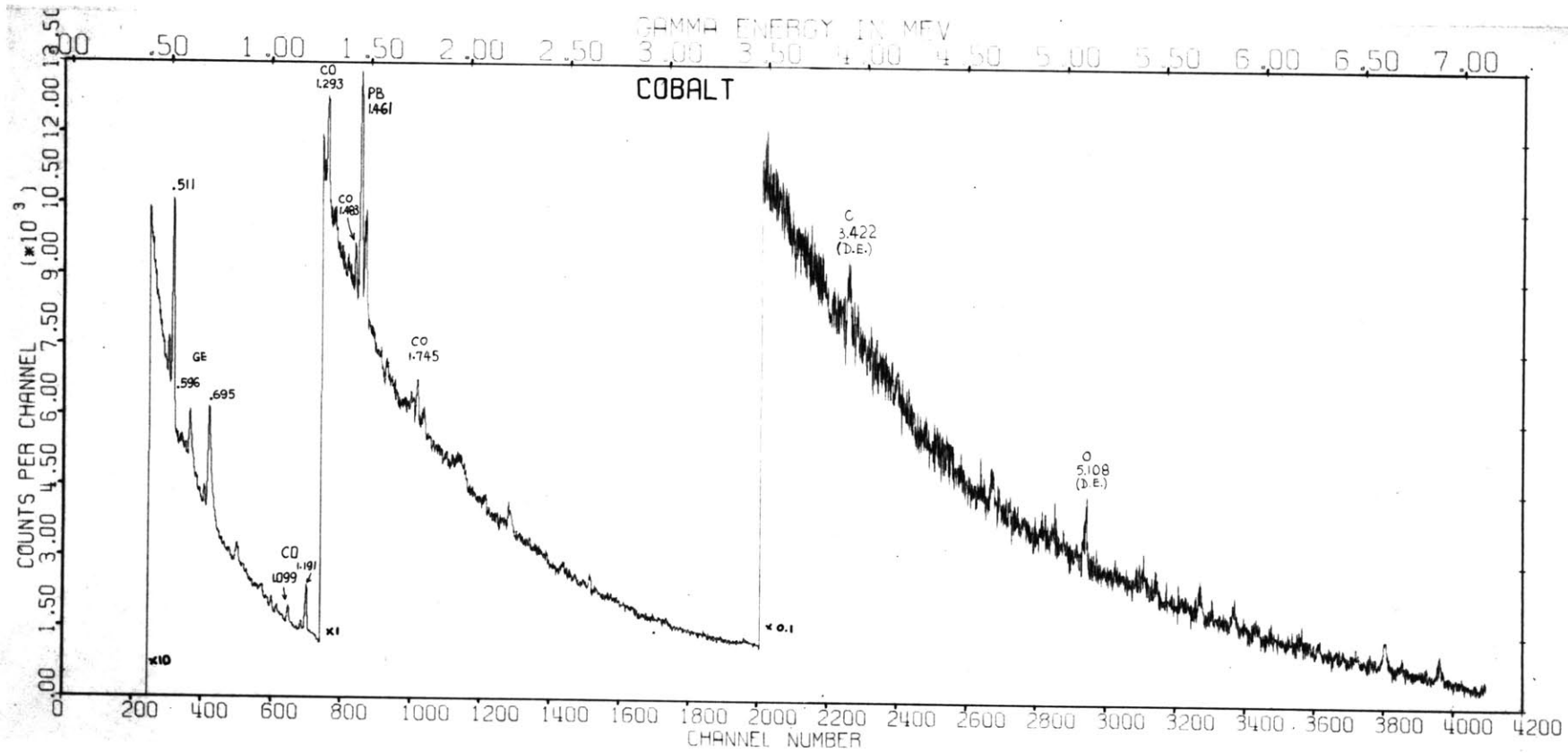
GAMMA ENERGY IN MEV
.00 .50 1.00 1.50 2.00 2.50 3.00 3.50 4.00 4.50 5.00 5.50 6.00 6.50 7.00
COBALT
CO 1.293
PB 1.461
CO 1.488
.511
GE .596
.695
CO 1.099
1.191
CO 1.745
C 3.422 (D.E.)
O 5.108 (D.E.)
×10
×1
×0.1
COUNTS PER CHANNEL (×10³)
0.00 1.50 3.00 4.50 6.00 7.50 9.00 10.50 12.00 13.50
0 200 400 600 800 1000 1200 1400 1600 1800 2000 2200 2400 2600 2800 3000 3200 3400 3600 3800 4000 4200
CHANNEL NUMBER

Figure 4.15

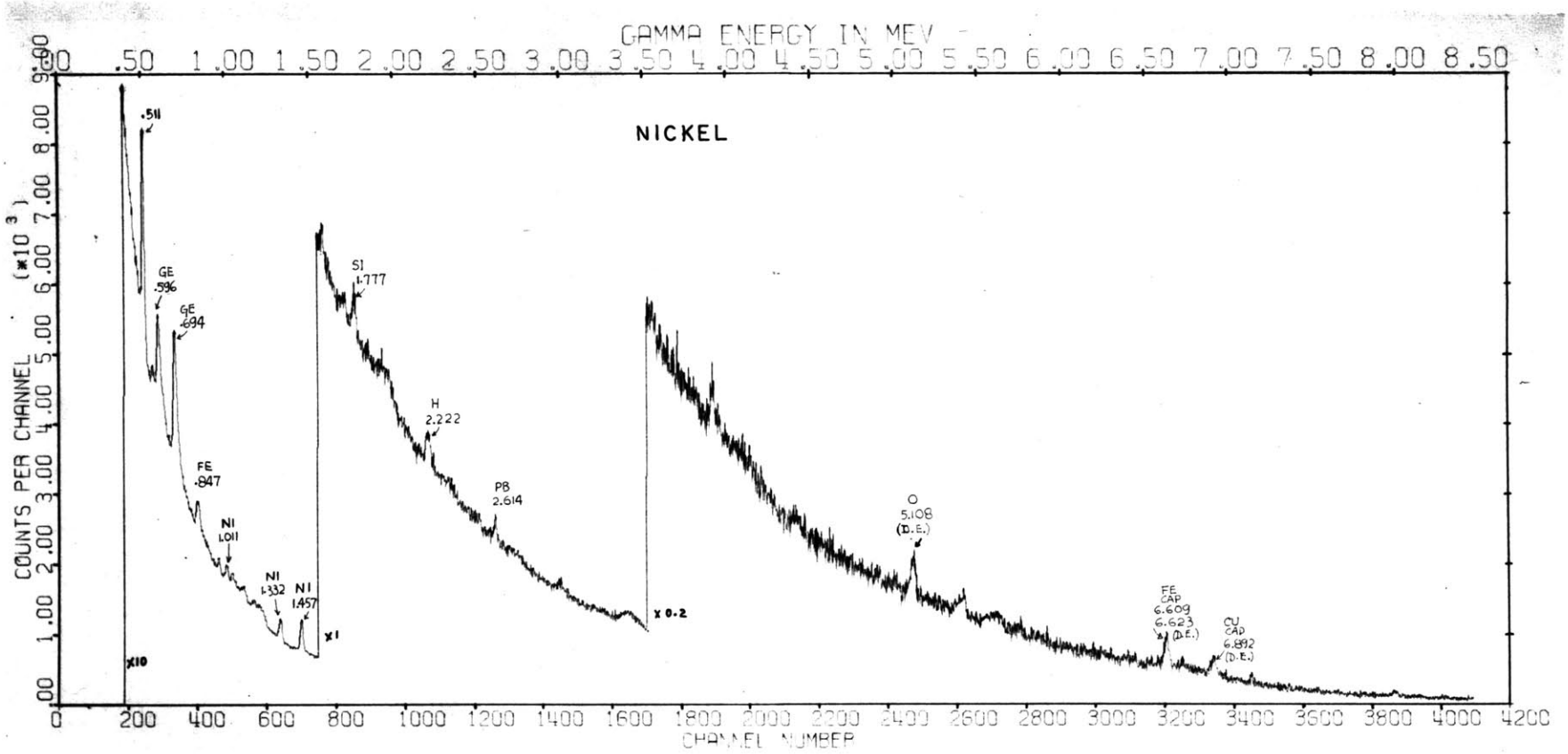
GAMMA ENERGY IN MEV
.00 .50 1.00 1.50 2.00 2.50 3.00 3.50 4.00 4.50 5.00 5.50 6.00 6.50 7.00 7.50 8.00 8.50
NICKEL
COUNTS PER CHANNEL (*10 3)
.00 1.00 2.00 3.00 4.00 5.00 6.00 7.00 8.00 9.00
.511
GE .596
GE .694
FE .847
NI 1.011
NI 1.332
NI 1.457
SI 1.777
H 2.222
PB 2.614
O 5.108 (D.E.)
FE CAP 6.609 6.623 (D.E.)
CU CAP 6.892 (D.E.)
x10
x1
x 0.2
0 200 400 600 800 1000 1200 1400 1600 1800 2000 2200 2400 2600 2800 3000 3200 3400 3600 3800 4000 4200
CHANNEL NUMBER

Figure 4.16

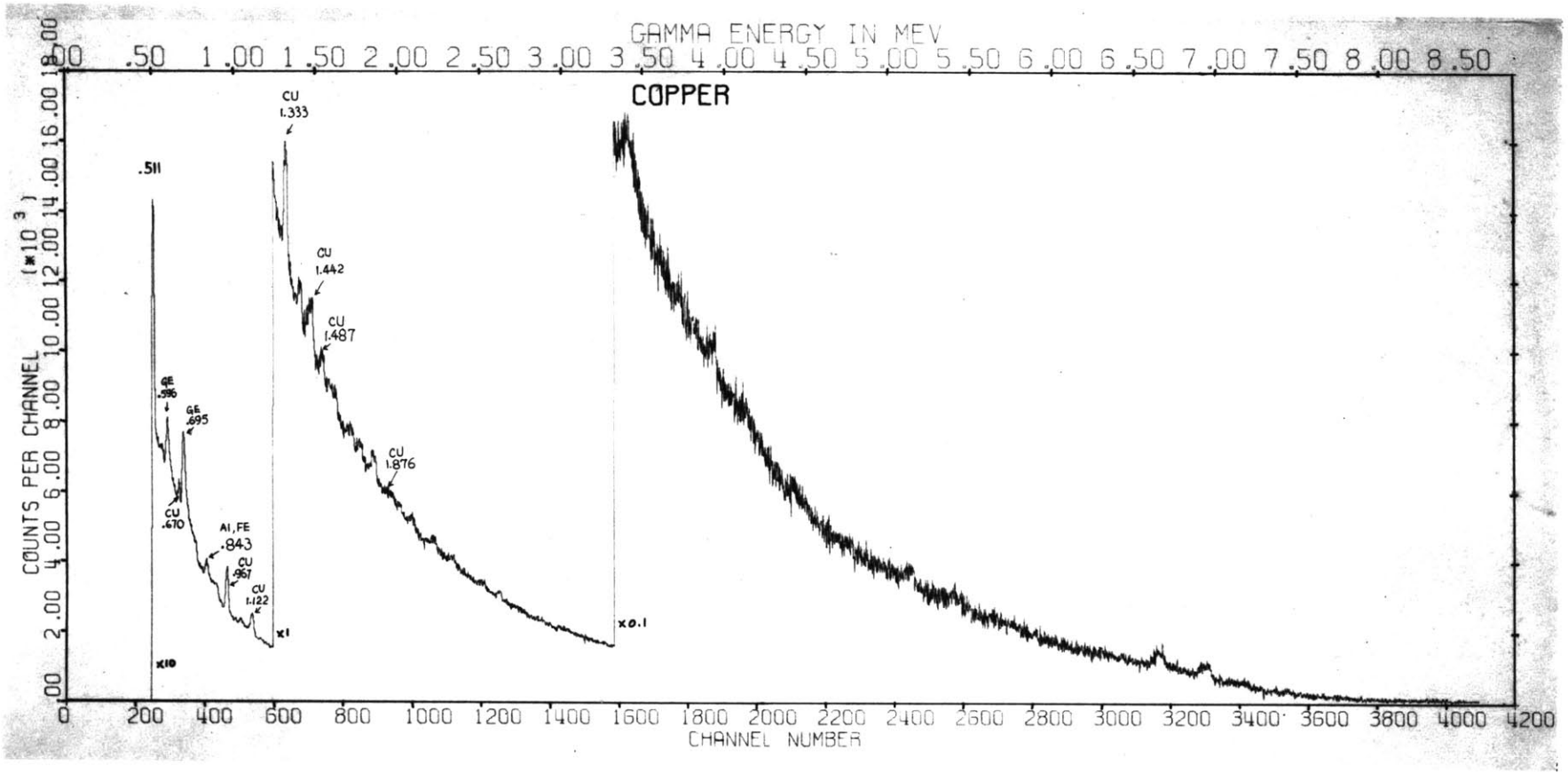
GAMMA ENERGY IN MEV
.00 .50 1.00 1.50 2.00 2.50 3.00 3.50 4.00 4.50 5.00 5.50 6.00 6.50 7.00 7.50 8.00 8.50
COPPER
COUNTS PER CHANNEL (*10^3)
.00 2.00 4.00 6.00 8.00 10.00 12.00 14.00 16.00 18.00
0 200 400 600 800 1000 1200 1400 1600 1800 2000 2200 2400 2600 2800 3000 3200 3400 3600 3800 4000 4200
CHANNEL NUMBER
.511
CU 1.333
CU 1.442
CU 1.487
CU 1.876
GE .596
GE .695
CU .670
AL,FE .843
CU .967
CU 1.122
x10
x1
x0.1

Figure 4.17

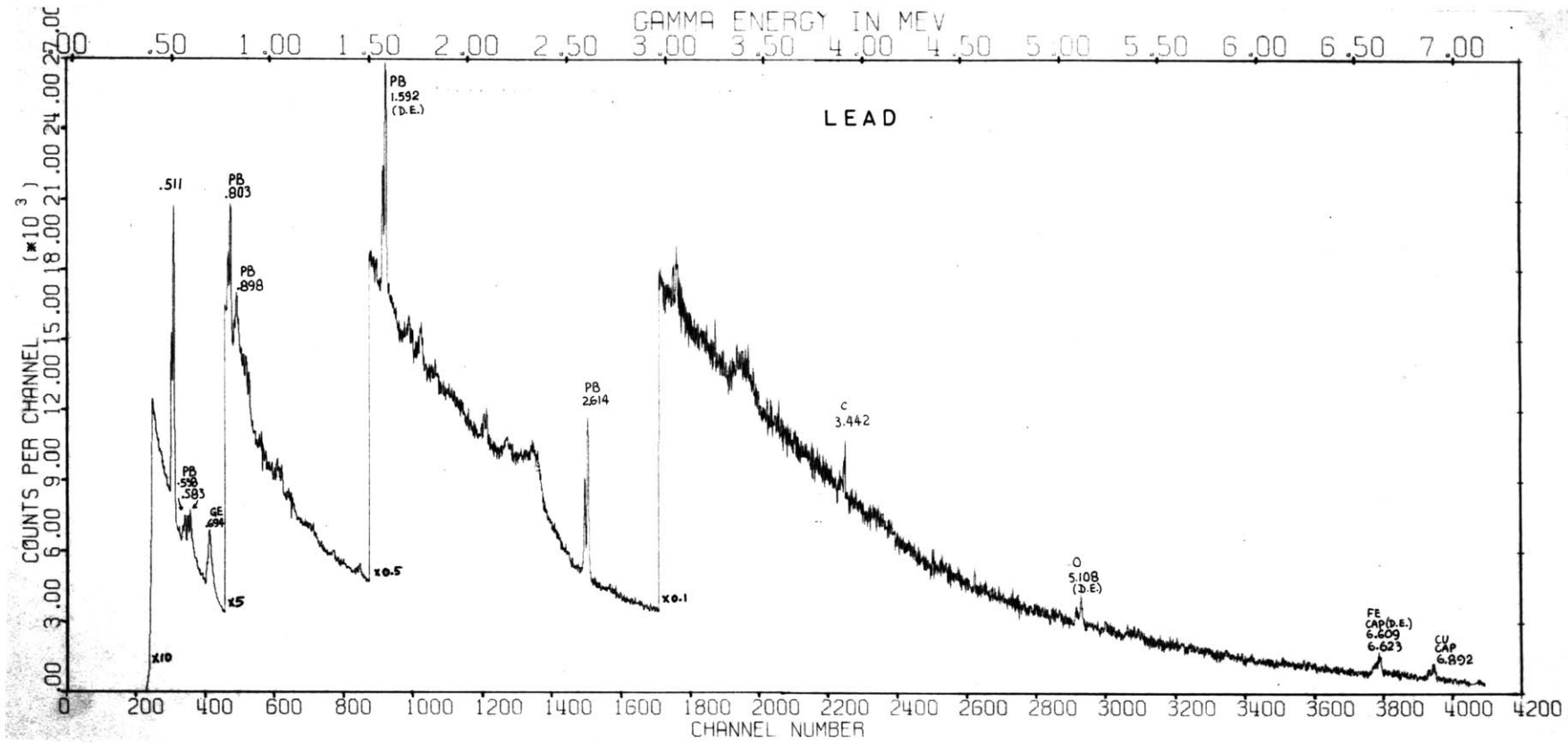
GAMMA ENERGY IN MEV
.00 .50 1.00 1.50 2.00 2.50 3.00 3.50 4.00 4.50 5.00 5.50 6.00 6.50 7.00
LEAD
COUNTS PER CHANNEL (*10 3)
.00 3.00 6.00 9.00 12.00 15.00 18.00 21.00 24.00 27.00
PB 1.592 (D.E.)
.511
PB .803
PB .898
PB .558 .583
GE .694
PB 2.614
C 3.442
O 5.108 (D.E.)
FE CAP(D.E.) 6.609 6.623
CU CAP 6.892
x10
x5
x0.5
x0.1
0 200 400 600 800 1000 1200 1400 1600 1800 2000 2200 2400 2600 2800 3000 3200 3400 3600 3800 4000 4200
CHANNEL NUMBER

Figure 4.18

energetically possible for it to undergo pair production where a positron and an electron are created. The positron will later annihilate with another electron to produce a pair of 0.511 MEV gamma rays. If these gamma rays escape without being detected, then the original gamma ray will appear at an energy 1.022 MEV less than $h\nu$. This peak is called the double escape peak of the original gamma ray. If only one of the 0.511 MEV gamma escapes and the other is detected, then the gamma ray will be only 0.511 MEV less and this peak is called the single escape peak. Usually the probability of detecting a single escape peak is small, so it will not be considered here.

The ratio between the intensity of double escape peak and the full energy peak is a function of the size of the detector crystal and gamma ray energy. Figure 4.19 shows this ratio vs energy for our detector. The data were obtained from a number of well known lines.

An unknown line in a spectrum was first checked whether it was a background line. If a line was within $\pm$ 5 KEV of a known background it was discarded. The remaining lines were then checked against Nuclear Data Sheets(ref. 7) to see if they fit the known nuclear levels of the element in question. In every case the strong lines in the spectra were found to agree within $\pm$ 10 KEV of known nuclear levels.

A line could also be the double escape line of another gamma ray. So after the above procedure, we added 1.022 MEV

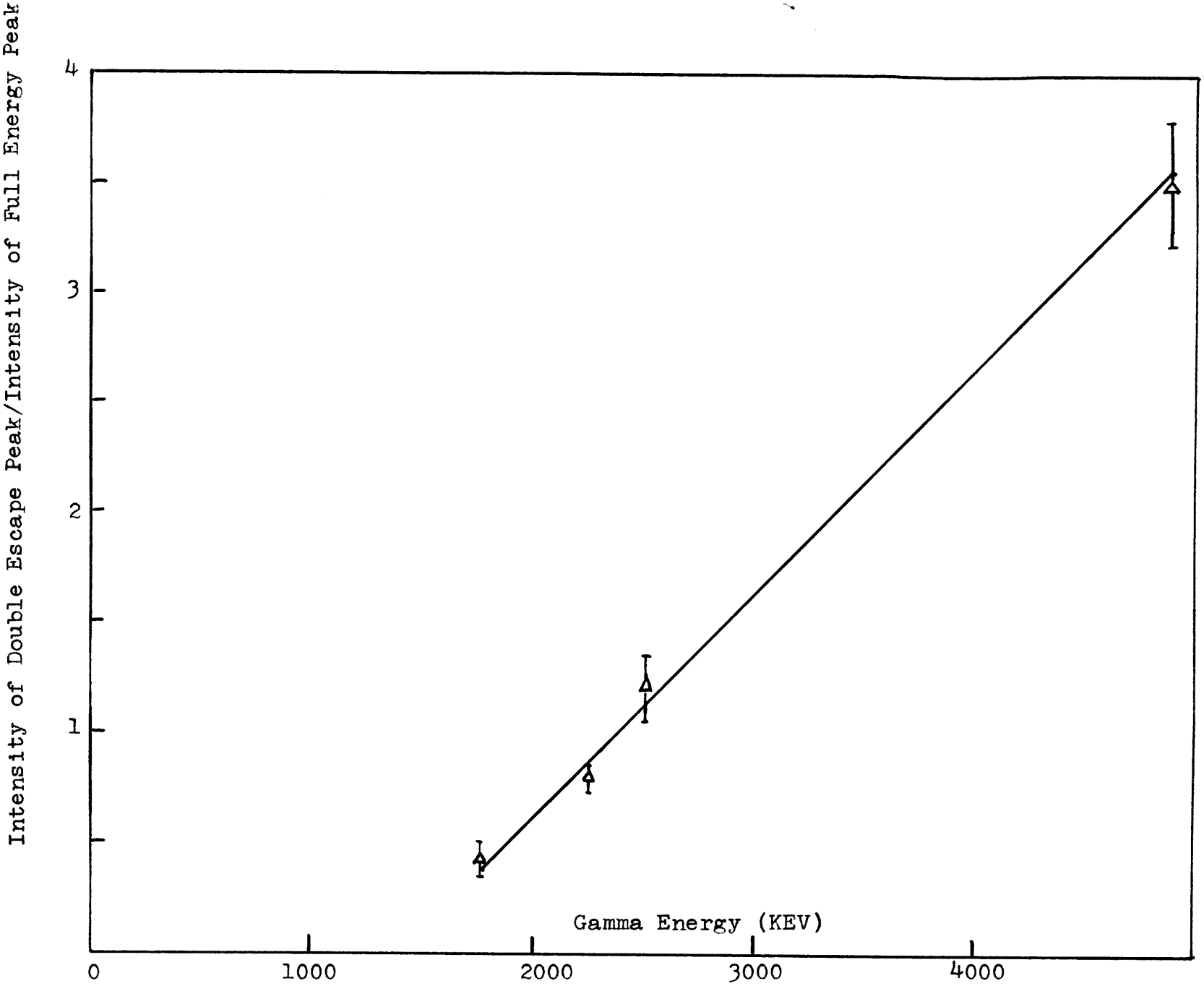

Figure 4.19 Ratio of Intensity of Double Escape Peak to Full Energy Peak

to the line and checked in our spectrum to see if there was such a full energy peak present. If there was such a line, we could still double check it with Figure 4.19 to see whether the ratio of the intensity of double escape peak to full energy peak fitted into our curve. It must be emphasized that the full energy peak generally did not show up at the high energies(above 3 MEV). A line above this energy was accepted if after adding 1.022 MEV to it corresponding to an inelastic gamma of an element. In this work all the high energy lines did meet this test.

For the twenty spectra, all gamma rays other than background with less than 20% error were identified and they fitted into the known level scheme. The results were shown in Table 4.3 . A number of weak lines could be seen in the spectra but in repeated runs it was determined that lines with errors greater than 20% could not be reliably identified and they have therefore not be included in the table.

4.3 Determination of Production Cross Section

To find the intensity of a gamma ray, we divided the area of that peak(column six, Table 4.1) by the run time, then subtracted its background intensity if it had any. The result was divided by the sample weight to yield intensity in counts per gram per min. This is shown in column three of Table 4.3 .

The above results were then used to calculate the

Table 4.3

Energy and Production Cross-section of Each Element

Element	Energy Kev (±5Kev)	Intensity (counts / min x gm)	Error	σ ± 50% barn
Lithium	479	0.459	3%	0.68
Carbon	4446 3935(SE) 3422(DE)	0.003	10%	0.02
Nitrogen	2317	0.2205	2%	3.33
Oxygen	*			
Magnesium	1369	0.029	3%	0.477
Aluminum	843	0.018	1%	0.17
	1014	0.024	2%	0.35
	1369	0.007	10%	0.01
	1722	0.003	6%	0.06
	1984	0.003	5%	0.09
	2212	0.005	2%	0.15
	2988 1963(DE)	0.0006	18%	0.01
Sodium	438	0.100	2%	0.54
	619	0.0188	5%	0.12
	1530(DE)	0.0017	32%	0.02
	2276	0.0003	38%	0.01
	2404 1383(DE)	0.0016	35%	0.03
	2663 1637(DE)	0.0053	15%	0.08
Silicon	1270	0.0001	20%	0.001
	1779	0.0096	6%	0.26
Sulphur	2225	0.0042	5%	0.14
Chlorine	1217	0.0019	15%	0.04
	1762	0.0020	11%	0.07

* The weight of oxygen in the sample cannot be determined accurately

DE, SE means Double or Single Escape, see page 51

Table 4.3 (contd.)

Element	Energy Kev (±5Kev)	Intensity (counts / min x gm)	Error	σ ± 50% barn
Potassium	2514	0.0008	20%	0.03
	2760 1732(DE)	0.0292	3%	1.03
	3593 2575(DE)	0.0018	30%	0.06
Titanium	889	0.0151	4%	0.25
	984	0.0712	2%	1.80
	1313	0.0089	4%	0.28
	1347	0.0009	24%	0.02
	1438	0.0015	10%	0.22
Vanadium	608	0.009	5%	0.49
	928	0.0066	28%	0.16
	1609	0.0091	4%	0.35
	1813	0.001	6%	0.04
Chromium	749	0.005	30%	0.09
	935	0.009	11%	0.21
	1434	0.030	2%	1.21
	1528	0.003	15%	0.12
Manganese	858	0.0133	8%	0.12
	1166	0.0011	46%	0.01
	1253(DE)	0.0006	19%	0.01
	1521	0.005	2%	0.11
	1880	0.002	3%	0.04
Iron	847	0.06	1%	1.20
	1237	0.008	2%	0.24
	1408	0.001	3%	0.16
	1810	0.003	3%	0.16
Cobalt	260	0.0734	3%	0.325
	381	0.005	8%	0.05
	555	0.0027	10%	0.02
	1099	0.005	4%	0.16
	1191	0.0148	3%	0.51
	1293	0.0032	4%	0.12
	1483	0.0031	4%	0.14
	1745	0.0013	6%	0.06

Table 4.3 (Contd.)

Element	Energy Kev (±5Kev)	Intensity (counts / min x gm)	Error	σ ± 50% barn
Nickle	1011	0.0019	8%	0.06
	1332	0.0117	3%	0.43
	1457	0.0157	2%	0.12
Copper	361	0.0041	5%	0.03
	670	0.0037	4%	0.05
	967	0.0032	8%	0.10
	1122	0.0072	5%	0.25
	1333	0.0047	10%	0.20
	1442	0.001	25%	0.003
	1487	0.004	53%	0.02
	1876	0.0002	17%	0.01
Lead	568	0.0017	20%	0.07
	583	0.0029	20%	0.13
	803	0.0038	10%	0.31
	898	0.0004	7%	0.03
	1063	0.0004	9%	0.05
	1366	0.0001	30%	0.01
	1822	0.0001	40%	0.02
	2614 1592 (DE)	0.0041	15%	0.91

production cross section using equation (2.10).

$$\sigma \approx \frac{2\pi P_D \ell_s^2}{\epsilon \phi_o N V} \qquad (4.1)$$

Usually for scrap samples, the volume is not known accurately because their irregular shape may leave lots of empty spaces inside the aluminum cans. It is better to use density rather volume. Dividing equation (2.10) top and bottom by the total sample weight, and recalling that V in eq. 4.1 is the volume of half of the sample, we get

$$\sigma \approx \frac{4\pi P_D' \ell_s^2 \rho}{\epsilon \phi_o N} \qquad (4.2)$$

where P_D' is measured in counts per minute per gram and ρ is the density of the sample. For our experimental setup, $\ell_s = 19.5 \pm 1$ cm, $\phi_o = 8 \times 10^6$ neutrons/sec, and N = atoms/cm^3. The efficiency $\epsilon = \epsilon_i g$ where ϵ_i is the intrinsic detector efficiency obtained from figure 3.2 and g, the geometric factor was calculated for this setup to be 3.22×10^{-4}. Using eq.(4.2) the production cross sections for different gamma rays were calculated and the results are shown in last column of Table 4.3. The $\pm 50\%$ error represents an approximate estimate of the accumulated errors in the measurement.

Chapter V

CONCLUSION

For our experiment, the inelastic gamma ray energies were accurate up to ± 5 Kev. Most of them were leas than 2 Mev. The production cross sections range from hundredth of a barn to a few barn.

The main source of error came from the efficiency curve, the non uniformity of neutron flux and the distance between the fast neutron source and the sample plate. It is estimated they contributed to an error of ± 50%.

The production cross section calculation shown in Chapter II is only good for thin slab geometry which assumes no gamma and neutron attenuation. However, in most practical cases, the sample is large and not necessarily a slab, in such case, it may be necessary to take both neutron and gamma ray attenuation into account.

Reference

1. R.F. Stewart, "Nuclear Measurements of Carbon in Bulk Materials", Transactions, ISA, v.6, No.3, September, 1967, pp 200-208

2. D.P. Simonson, "Promp Gamma Ray Spectra Produced By Neutrons From A Pu-Be Source", S.M. Thesis, August 1968, M.I.T.

3. V.J. Orphan and N.C. Rasmussen, "Study of Thermal Capture Gamma Rays Using a Lithium-Drifted Germanium Spectrometer", Report No. MITNE-80, January, 1967

4. T. Harper, T. Inouye, N.C. Rasmussen, "GAMANL- A Computer Program Applying Fourier Transforms to the Analysis of Gamma Spectra Data." Report No. MITNE-97 August, 1968

5. J.N. Hamawi, "Investigation of Elemental Analysis Using Neutron Capture Gamma Ray Spectra", Ph.D. Thesis September, 1969

6. T.L. Harper Jr., "Determination of Thermal Neutron Capture Gamma Yields", Report No. MITNE-104 July, 1969

7. N.B. Gove, editor, Nuclear Data Sheets, Vol. 5, November, 1963